9 Marine Carbonates: Their Formation and Destruction

Ralph R. Schneider, Horst D. Schulz and Christian Hensen

9.1 Introduction

For marine carbonates, an overwhelming amount of information exists in a variety of specialized journals addressing marine geochemistry and carbon cycling, as well as in many books summarizing the state of knowledge on this topic. Therefore it would be far beyond the scope of this chapter to try to completely review what is known about marine calcareous sediments and their diagenesis. On the other hand, although intensively investigated since the previous century (e.g. Murray 1897), marine carbonates have gained increasing attention by marine biologists, geochemists, paleoceanographers and paleoclimatologists over the last three decades. Among other reasons this is because marine carbonates, together with the oceanic CO_2-carbonic acid-system, act as a sink or source of carbon within the global carbon cycle which has become a key topic of investigation and modelling related to the role of the greenhouse gas CO_2 in future global climate change.

Descriptions of sedimentary carbonates in different oceanic environments always have dealt with the formation of the calcium carbonate and the biologically, physically and chemically mediated processes governing the observed distribution of sedimentary carbonates in the marine realm. In this context special emphasis was often given to the complex pattern of inorganic and organic carbon exchange between the atmosphere, the world ocean and the continents. These are additional factors determining the distribution of inorganic carbon dissolved in seawater and the accumulation or destruction of calcium carbonate in marine sediments (Berger 1976; Andersen and Malahoff 1977; Broecker and Peng 1982; Sundquist and Broecker 1985; Morse and Mackenzie 1990). The intention of this chapter is furthermore to review the knowledge on the rate of calcium carbonate production in the ocean, the fluxes through the water column, as well as the rates of inorganic carbon accumulation and destruction in different marine environments. For this purpose this chapter summarizes studies dealing with the estimation of global carbonate reservoirs and fluxes in the state of ongoing production, accumulation and dissolution or physical erosion (Milliman 1993; Milliman and Droxler 1996; Wollast 1994). In addition, this chapter addresses the principles and presents examples for calculation of carbonate saturation conditions under variable boundary conditions in the oceanic CO_2-carbonic acid-calcite system, i.e. temperature, pressure, salinity, and CO_2 exchange with the atmosphere.

9.2 Marine Environments of Carbonate Production and Accumulation

This section primarily focuses on the description of the deposition and accumulation of carbonates in shallow waters and in the deep ocean. The main depocenters for calcium carbonates are the continental shelf areas, as well as island arcs or atolls, which are the typical shallow water environments for massive carbonate formation, and the pelagic deep-sea sediments above the calcite compensation depth catching the rain of small calcareous tests formed by marine plankton in the surface waters.

9.2.1 Shallow-Water Carbonates

Shallow-water carbonates are formed either by sediments made up of a variety of carbonate par-

ticles which have their origin in biotic and abiotic processes, or by massive reefs and platforms built up by skeleton-forming organisms. On a global scale, these shallow-water carbonates in the modern environment are mainly constituted by particles of skeletal origin. However, aside from the corals, the understanding of the physico-chemical and vital factors affecting the biomineral composition of shallow platform calcareous sediments in warm waters is still incomplete. Shallow environment precipitates form ooids and aragonitic needle muds, whereby the former involve primarily abiotic processes and the latter have both an abiotic and biotic source.

For long time, the classical picture of shallow water carbonates was suggesting that most of their formation was restricted to tropical and subtropical regions within the 22°C isotherm of annual mean surface water temperatures (e.g. Berger and Seibold 1993), but it now has become evident that a significant amount of carbonate can also be formed as so-called 'cool-water' carbonate banks and reefs in temperate and cold latitudes (review by James 1997; Freiwald 2002). In the temperate and cold-water zones, particularly shelf and upper slope areas with only very low inputs of terrigenous sediments are covered by cool-water carbonate bioherms (Fig. 9.1a). Different from the warm-water environment, where the major portion of skeletal carbonate is predominantly formed by an association of hermatypic corals and green algae referred to as '*Photozoan Association*' (James 1997), the cool-water carbonates can be composed of molluscs, foraminifers, echinoderms, bryozoans, barnacles, ostracods, sponges, worms, ahermatypic corals and coralline algae. For differentiation from the warm-water *Photozoan Association*, the group of organisms forming cool-water carbonates in shallow waters that are colder than 20°C is defined by James 1997 as *Heterozoan Association* (see also Fig. 9.1). According to Freiwald (2002) the largest coral reef provinces occur at greater water depths under cold and dark conditions usually below the storm wave base from the high to low latitudes of both hemispheres. In the North Atlantic the dominant reef-forming corals belong to scleractinian species. A first attempt to calculate the amount of $CaCO_3$ produced by cold-water reefs on global carbonate production was provided by Lindberg & Mienert (2005). Their estimate is in the order of 4 to 12 % of that of tropical reefs which results in a tentative estimate > 1 % of total marine carbonate production. Since these first estimates are relying on data from the Norwegian shelf only, it is difficult to come up with really reliable global carbonate production esti-mates for cold-water reefs at the moment. Therefore the estimates of Wollast (1994); Milliman & Droxler (1996), and Vecsei (2004) for worldwide shelf areas are considered here. For budget considerations it seems feasible to separate shal-low-water carbonates according to Milliman (1993) into coral reefs, carbonate platforms which consist of non-reef habitats, such as banks and embayments dominated by the sedimentation of biogenic and abiogenic calcareous particles, and shelves which can be further subdivided into car-bonate-rich and carbonate-poor shelves (Table 9.1 adopted from Milliman (1993) and Milliman and Droxler (1996), taking into account Vescei (2004) estimates.

Reefs

Hermatypic coralalgal reefs and their fore-reef sections occupy an area of about $0.35 \cdot 10^6$ km^2 and are considered as the most productive carbonate environments in modern times. Carbonate accretion is the result of corals and green algae and, to a minor extent also of benthic foraminifera. Measured on a global scale, the mean calcium carbonate accumulation in coral reefs is in the order of 900-2700 g $CaCO_3$ m^{-2}yr^{-1}. The total present-day global $CaCO_3$ production by coral reefs then is 6.5-8.3 $\cdot 10^{12}$ mol yr^{-1} from which about $7 \cdot 10^{12}$ mol yr^{-1} accumulate, while the rest (up to $1.5 \cdot 10^{12}$ mol yr^{-1}) undergoes physical erosion and offshore transport, as well as biological destruction (Milliman 1993).

Carbonate platforms

These platforms are the second important tropical to subtropical environment where high amounts of carbonate are produced and accumulated at water depths shallower than 50 m. The areal extension is about $0.8 \cdot 10^6$ km^2. In contrast to reefs, on carbonate platforms production is mainly carried out by benthic red/green algae, mollusks and benthic foraminifera. Estimates of biotic and, to a much lesser extent, abiotic carbonate production on platforms range between 300-500 g $CaCO_3$ m^{-2} yr^{-1}, which amounts to $4 \cdot 10^{12}$ mol yr^{-1} on a global scale. Accumulation of platform carbonate is difficult to assess because a lot of it is dissolved or can be found as exported material in several 10 to 100 m

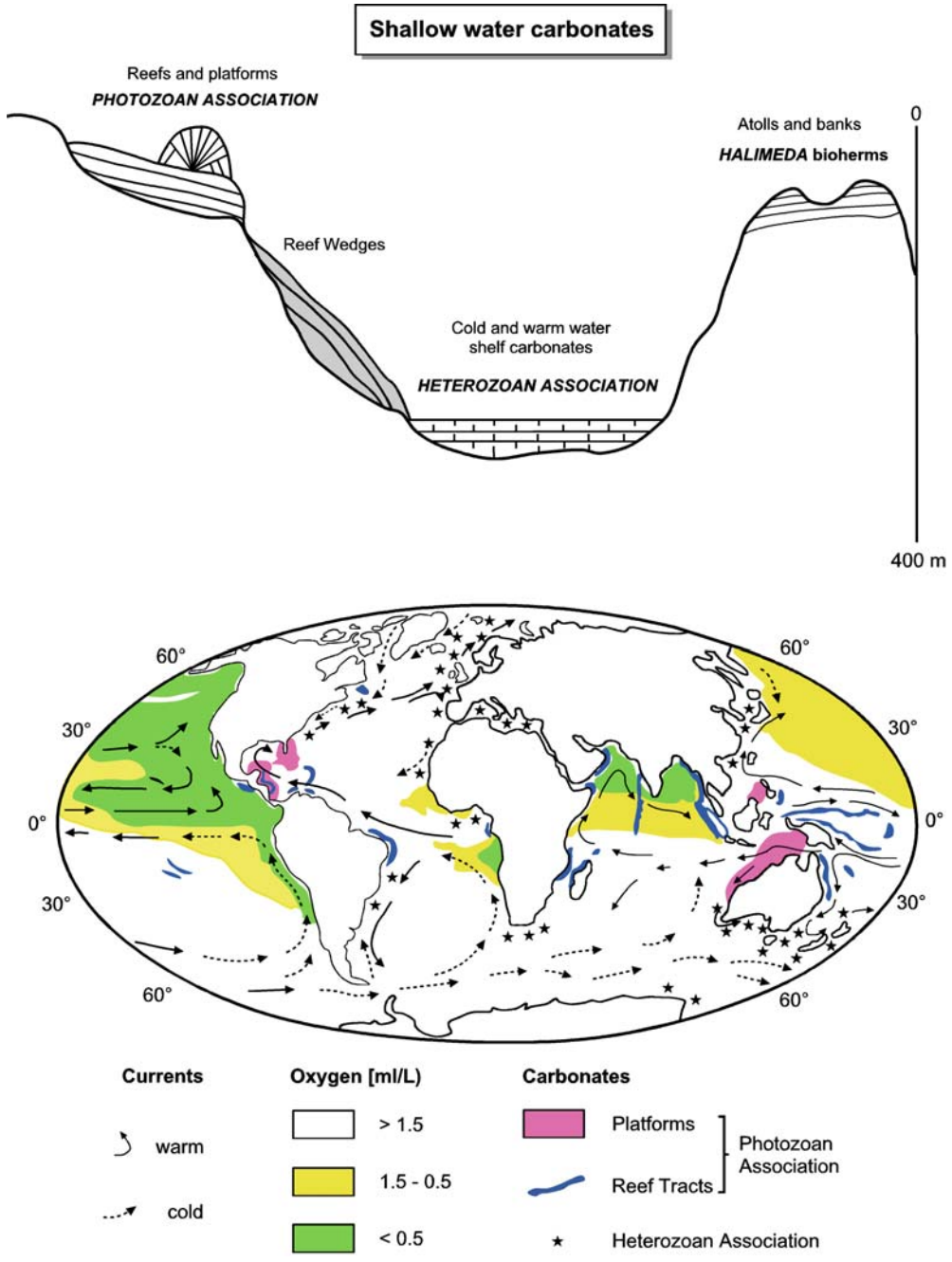

Fig. 9.1 Marine calcium carbonate accumulation in a) typical depocenters in shallow waters and b) their global distribution (James and Clarke 1997).

thick sediment wedges of Holocene age at the fringes of the platforms. Milliman (1993) estimates that only one half of the carbonate accumulates on shallow platforms where it is produced ($2 \cdot 10^{12}$ mol yr^{-1}), while the other half leaves the shallow water environment in the form of sediment lobes or wedges downslope.

Continental shelves

Only very little knowledge exists concerning the quantitative carbonate production, export and its accumulation on continental shelves. Two shelf types, carbonate-rich and carbonate-poor shelves, are distinguished by Milliman and Droxler (1996).

Their areas amount to 15 and $10 \cdot 10^{12}$ km^2, respectively (Hay and Southam 1977). However for the two shelf types well-constrained estimates of how much carbonate is produced are missing. In the context of shelves it may be important to separate two other specific bioherms which could have a great potential in shallow-water carbonate production. These are sedimentary carbonates exclusively built up by the calcareous green algae *Halimeda* in tropical latitudes (e.g. Roberts and Macintyre 1988) and extensive biotic cold-water carbonate reefs or banks as described above for mid to high latitudes. For *Halimeda* bioherms total carbonate production and accumulation is about $1.5 \cdot 10^{12}$ mol yr^{-1} (Table 9.1) while the estimates for open shelves given by Wollast (1994) and Milliman and Droxler (1996) do not differentiate a budget for cold-water shelf areas on its own. Mean carbonate production on lower-latitude shelf areas may range between 50 and 100 g m^{-2}yr^{-1} (Table 9.1); in total $6 \cdot 10^{12}$ mol yr^{-1}. How much of this annual production actually accumulates, is dissolved or exported to the deep-sea remains questionable, because shelf sediments are commonly a mixture of modern and relictic components. Moreover, accumulation rates on broad sandy shelves like that off Argentina are not well-known, because they have not been investigated in such detail yet as other shelf environments. According to Milliman and Droxler (1996) half of the production on carbonate-rich shelves is accumulating ($3 \cdot 10^{12}$ mol yr^{-1}; Table 9.1) while the other half is either transported downslope to the deep sea or dissolved. For carbonate-poor shelves carbonate

Table 9.1 Maximum estimates of present-day carbonate production and accumulation. The difference between production and accumulation is taken as an estimate for dissolution (after Milliman 1993, Milliman and Droxler 1996, Vescei 2004). All numbers labeled with ? are supposed to have an possible error of greater than 100 %.

Habitat	Area ($\cdot 10^6$ km^2)	$CaCO_3$ Production (g m^2 yr^{-1})	$CaCO_3$ Production (10^{12} mol yr^{-1})	Accumulation (10^{12} mol yr^{-1})	Dissolution/Erosion (10^{12} mol yr^{-1})
Shallow waters:					
Coral Reefs	0.35	1800	9	7	2
Platforms	0.8	500	4	2	2
Shelves:					
Carbonate-poor	15	25 ?	4 ?	1 ?	3 ?
Carbonate-rich	10	20-100 ?	6 ?	3 ?	3 ?
Halimeda bioh.	0.05 ?	3000 ?	1.5 ?	1.5 ?	
Total Shallow-water carbonates			**24.5**	**14.5**	**10**
Deep Sea:					
Slopes	32	15	5	4	1
(improved from shelfes)			3.5 ?	2	1.5
Pelagic Surface Waters	290	23	60-90		
(Flux at 1000m		8		24	36 ?)*
Sea floor				11-19	5-13 (in the deep waters & surficial sediments)
Total Deep-sea carbonates			**68.5-90 ?**	**17-25**	**51.5-67**

* Problem of very low fluxes at 1000 m water depth estimated from sediment trap data. Implies very high dissolution rates above the lysocline.

production should at least exceed 20 g $m^{-2}yr^{-1}$ which is the average value of planktonic production in coastal waters. While global carbonate production on carbonate-poor shelves may be relatively high ($4 \cdot 10^{12}$ mol yr^{-1}; Milliman and Droxler 1996), carbonate accumulation in this environment is negligible.

The rate of total neritic carbonate production in the modern ocean is roughly $25 \cdot 10^{12}$ mol yr^{-1} from which 60 % ($15 \cdot 10^{12}$ mol yr^{-1}) accumulate as shallow-water carbonates. The difference, $10 \cdot 10^{12}$ mol yr^{-1}, is the contribution of the neritic environment to the pelagic environment, either in the form of flux of total dissolved inorganic carbon or particulate accumulation on continental slopes and in the deep sea.

9.2.2 Pelagic Calcareous Sediments

Calcium carbonate is the most important biogenic component in pelagic marine sediments which cover an area of about $320 \cdot 10^6$ km^2. Carbonate-rich sediments (>30 % $CaCO_3$) form about 55 % of the deposits on the continental slopes and the deep-sea floor (Lisitzin 1996; Milliman 1993). A new compilation on the distribution of carbonate-rich pelagic sediments (Fig. 9.2b) has been recently carried out by Archer (1996a).

The distribution of pelagic marine carbonates is a result of a variety of influences. The most important components of the pelagic carbonate system affecting their formation and destruction are shown in Figure 9.2b. These can be divided in external contributions such as riverine input and CO_2-exchange with the atmosphere and the lithosphere (hydrothermal venting), and internal processes. The main internal processes are those by which $CaCO_3$ is produced and dissolved in the ocean. In the pelagic realm carbonate is mainly produced by planktonic organisms in ocean surface waters supersaturated with calcite and aragonite. Production of biogenic calcite or aragonite comes from planktonic organisms like coccolithophorids, foraminifers and pteropods, as well as calcareous dinoflagellates. The amount of the total production is determined by temperature, light, and nutrient-conditions in the surface ocean. On upper slopes, where food supply is high, part of the carbonate production also originates from benthic foraminifera and small mollusks. Estimates of the global calcium carbonate production by pelagic organisms are difficult to assess, because the amount of production per unit of water volume or area cannot be directly measured. In addition, according to sparse data available from plankton hauls and shallow floating trap catchments they vary significantly between oligotrophic and eutrophic, and particularly between silicon-poor and silicon-rich surface waters (Fischer et al. 2004). Mean global estimates are either derived from sediment trap fluxes at about 1000 m water depth (Milliman 1993) or from theoretical approaches in which the production required to explain the observed water-column profiles of alkalinity and total dissolved inorganic carbon (Fig. 9.3) is calculated, taking the modern ocean circulation pattern and residence times of the different water masses into account. However, these estimates differ by a factor of two to three, whereby the sediment trap data and surface-water properties suggest a mean global calcium carbonate production of 23 or 60 to $90 \cdot 10^{12}$ mol yr^{-1}, respectively (see comments and discussion in Morse and Mackenzie 1990; Milliman and Droxler 1996; Wollast 1994).

How much of the carbonate produced in the surface ocean finally accumulates on the sea floor and is buried there, depends on the calcite dissolution in the water column during the settling of particles and on the calcite dissolution within the sediment. For slope sediments also dilution with sedimentation of terrigeneous material affects the carbonate content. Dissolution of pelagic carbonates is driven by the aragonite and carbonate saturation levels in the deep-sea, controlled by temperature and pressure conditions, as well as by pH and alkalinity of circulating deep-water masses (Berger 1976; Broecker and Peng 1982). On its way to the deep sea the settling biogenic carbonate reaches waters which are increasingly undersaturated with respect to aragonite and later calcite, due to the decrease in temperature, increases of pressure, and the latter CO_2 resulting from the reoxidation of organic matter. Increase of CO_2 due to benthic respiration also affects $CaCO_3$ which reaches the sea floor. Early diagenesis forces calcite dissolution in the upper sediment column even at supralysoclinal and lysoclinal water depths due to excess pore water CO_2 originating from remineralization of sedimentary organic matter (Archer 1991, 1994; Jahnke et al. 1994; Martin and Sayles 1996). The latter will be discussed in more detail in Section 9.4. Moreover, the ocean's circulation also changes the depth distribution of water masses with different saturation levels of aragonite and calcite. As a consequence, only a small fraction

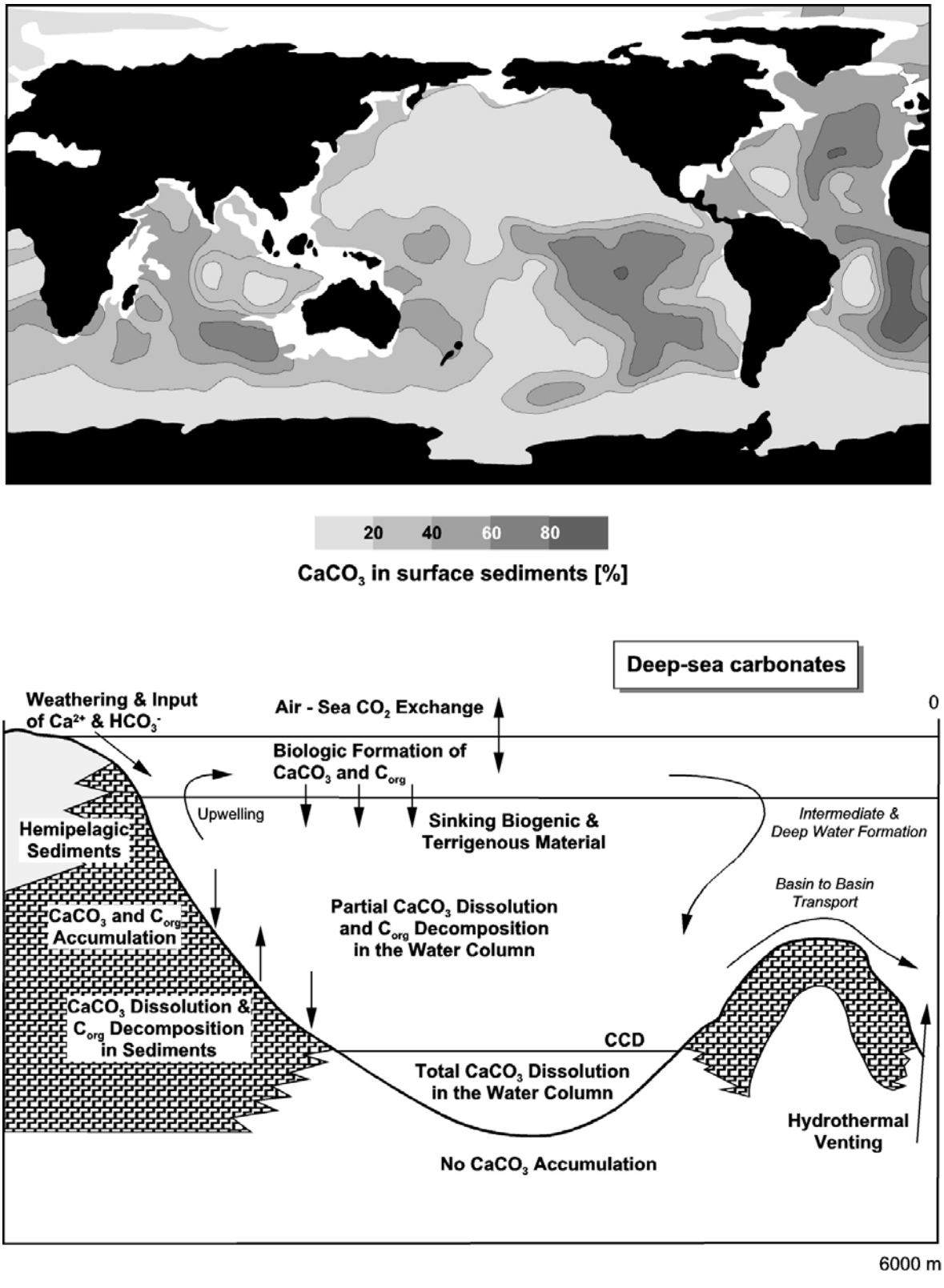

Fig. 9.2 Environments of pelagic carbonate deposition: a) deep-sea distribution of carbonate-rich sediments (new compilation from Archer 1996a) and b) factors controlling pelagic carbonate production and dissolution (modified from Morse and Mackenzie 1990).

(15 to 20 %; see Table 9.1, or Archer 1996b, Wollast 1994) of the total amount of pelagic carbonates produced in the upper ocean is buried in deep-sea sediments. Different estimates for mean global calcium carbonate accumulation rates from various authors (Milliman 1993; Morse and Mackenzie 1990; Wollast and Mackenzie 1987) are in good agreement for the deep sea, all ranging between $10 \cdot 10^{12}$ mol yr^{-1} and $12 \cdot 10^{12}$ mol yr^{-1} (1 to 1.2 bt $CaCO_3$ yr^{-1}).

Essentially all the above mentioned factors have the potential to change the calcite-carbonate equilibrium in the ocean over time and thus exert major control on the distribution and amount of calcareous sediments in the deep sea. On the other hand, given the 60 times greater carbon reservoir of the ocean compared to that of the atmosphere, changes in the oceanic calcite-carbonate equilibrium can modify the oceanic CO_2 uptake/release balance with respect to the atmosphere (Archer and Maier-Reimer 1994; Berger 1982; Broecker and Peng 1987; Maier-Reimer and Bacastow 1990; Opdyke and Walker 1992; Siegenthaler and Wenk 1984; Wolf-Gladrow 1994; see also review in Dittert et al. 1999). Therefore, the principles of the calcite-carbonate system will be re-examined in the following Section 9.3 and examples will be given for modeling this system under specific boundary conditions typical for the modern ocean. As we know from the geological record of calcareous sediment distribution, this system has changed dramatically in the past and definitely will change in the future, leaving us with the questions of how much, how fast and in which direction the ocean carbonate system will respond to anthropogenic disturbances of the carbon cycle in the future, which may result in a more acid ocean (Feely et al. 2004, Orr et al. 2005).

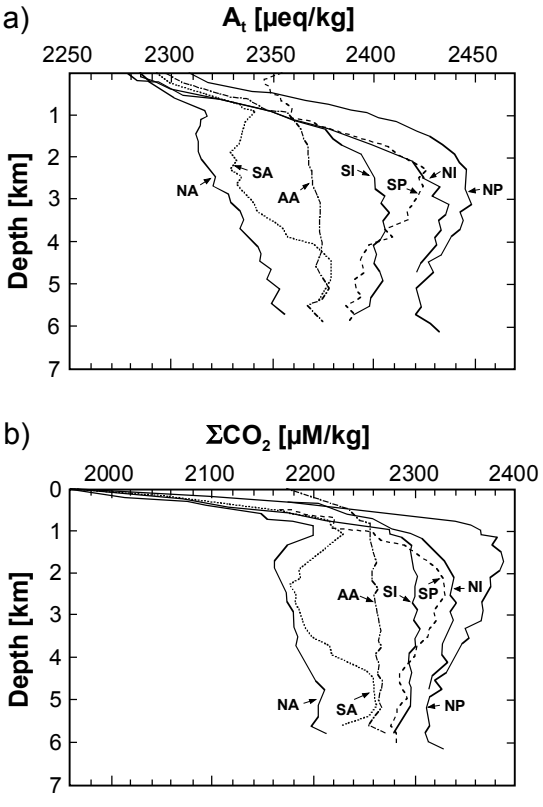

Fig. 9.3 The mean vertical distribution of a) alkalinity and b) total CO_2 concentration normalized to the mean world ocean salinity value of 34.78 (after Takahashi et al. 1980, adapted from Morse and Mackenzie 1990)

9.3 The Calcite-Carbonate-Equilibrium in Marine Aquatic Systems

The calcite-carbonate-equilibrium is of particular importance in aquatic systems wherever carbon dioxide is released into water by various processes, and wherever a concurrent contact with calcite (or other carbonate minerals) buffers the system by processes of dissolution/precipitation. Carbon dioxide may either originate from the gaseous exchange with the atmosphere, or is formed during the oxidation of organic matter. In such a system this equilibrium controls the pH-value - an essential system parameter which, directly or indirectly, influences a number of secondary processes, e.g. on iron (cf. Chap. 7) and on manganese (cf. Chap. 11). In the following, the calcite-carbonate equilibrium will be described in more detail and with special attention given to its relevant primary reactions.

The description of Sections 9.3.1 and 9.3.2 will assume in principle a solution at infinite dilution in order to reduce the system to really important reactions. The Sections 9.3.3 and 9.3.4 provide examples calculated for seawater, including all constituents of quantitative importance. In such calculations, two different approaches are possible:

The use of measured concentrations (calcium, carbonate, pH) together with so-called 'apparent' equilibrium constants. These apparent constants (e.g. Goyet and Poisson 1989; Roy et al. 1993; Millero 1995) take the difference between activities and concentrations into account, as well as

the fact, that for instance only part of the measured calcium is present in the form of Ca^{2+}-ions, whereas the rest forms complexes or ion pairs ($CaSO_4{}^0{}_{aq}$, $CaHCO_3{}^+{}_{aq}$, or others). This is true for seawater, since the activity coefficients of these complexes or ion pairs with sufficient accuracy exert a constant influence.

The other approach employs a geochemical computer model, such as PHREEQC (Parkhurst 1995; also Chap. 15) with an input of a complete seawater analysis. Such a model will then calculate the activity coefficients and the species distribution of the solution according to the complete analysis and the constants of the thermodynamic database used. These constants are well known with an accuracy which is usually better than the accuracy of most of our analyses at least for the major aquatic species. Together with the 'real' constant of the solubility product a reliable saturation index (SI = log Ω) is then calculated. The constants of solubility products are not accurately known for some minerals, but for calcite, and also for most other carbonates, these constants and their dependence on temperature and pressure are very well documented.

Both approaches used in the analysis of seawater lead to identical results, thus leaving it undetermined which method should be preferred for seawater analysis. However, for marine pore water the first approach is *not valid*, since quite different concentrations of complexes or ion pairs are likely to occur, for instance, sulfate reduction and/or an increase of alkalinity. Therefore we rely on the second approach in our examples and strongly recommend it for the marine geochemistry.

9.3.1 Primary Reactions of the Calcite-Carbonate-Equilibrium with Atmospheric Contact in Infinitely Diluted Solutions

Upon making contact with the atmosphere, the partial pressure (pCO_2) of carbon dioxide ($CO_{2,g}$) determines the concentration of carbonic acid ($H_2CO^0{}_{3,aq}$) in solution. The equilibrium reaction is written as:

$$CO_{2,g} + H_2O \Leftrightarrow H_2CO_3{}^0{}_{aq} \qquad (9.1)$$

The equilibrium is determined by the equation:

$$K_{CO2} = [H_2CO_3{}^0{}_{aq}] / \{pCO_2 \cdot [H_2O]\} = 3.38E\text{-}2 \quad (25^\circ C, 1\ atm) \qquad (9.2)$$

In this form the reaction combines two different steps: One leads to the formation of $CO_{2,aq}$ in aqueous solution, and a second leads from $CO_{2,aq}$ to the formation of $H_2CO_3{}^0{}_{aq}$. The brackets [...] denote activities, whereas parentheses embrace molar concentrations. The activity of water [H_2O] is equal to 1.0 in infinitely diluted solutions, whereas it is slightly less in seawater (0.981). The value of the constant K_{CO2} – as for all other constants in the following – is determined at a temperature 25°C and under a pressure of 1 atm. The temperature dependency of the constants was empirically investigated by Plummer et al. (1978) for the range between 5°C and 60°C. The computer program PHREEQC (Parkhurst 1995) also accounts for this temperature dependence. The pressure dependence, which is important in great water depths, is considered only in the model SOLMINEQ (Kharaka et al. 1988). The constants belonging to this program, corrected for specific water depths, can be extracted and explicitly entered into the database of the generally more versatile model PHREEQC.

The aqueous complex $H_2CO_3{}^0{}_{aq}$ dissociates into protons and bicarbonate ions:

$$H_2CO_3{}^0{}_{aq} \Leftrightarrow H^+ + HCO_3^- \qquad (9.3)$$

This equilibrium is described by the equation:

$$K_{H2CO3} = \{[H^+] \cdot [HCO_3^-]\} / [H_2CO_3{}^0{}_{aq}] = 4.48E\text{-}7 \quad (25^\circ C, 1\ atm) \qquad (9.4)$$

The second step of dissociation is determined by:

$$HCO_3^- \Leftrightarrow H^+ + CO_3^{2-} \qquad (9.5)$$

This equilibrium is described by the equation:

$$K_{HCO3} = \{[H^+] \cdot [CO_3^{2-}]\} / [HCO_3^-] = 4.68E\text{-}11 \quad (25^\circ C, 1\ atm) \qquad (9.6)$$

Furthermore, the dissociation of water needs to be included:

$$H_2O \Leftrightarrow H^+ + OH^- \qquad (9.7)$$

with the constant K_{H20}:

$$K_{H2O} = [H^+] \cdot [OH^-] = 1.00E\text{-}14 \quad (25^\circ C, 1\ atm) \qquad (9.8)$$

The contact made by processes of dissolution and precipitation with the solid phase of calcite is described by the reaction:

$$CaCO_{3,calcite} \Leftrightarrow Ca^{2+} + CO_3^{2-} \qquad (9.9)$$

The equilibrium is described by the equation:

$$K_{calcite} = [Ca^{2+}] \cdot [CO_3^{2-}] = 3.31E\text{-}9 \quad (25^{\circ}C, 1\ atm) \qquad 9.10$$

Another essential condition for describing the calcite-carbonate-equilibrium consists in the fulfillment of the neutral charge rule. This holds that charges may be neither lost nor gained on reaching the equilibrium state.

The balance of the charges is done indirectly on the basis of the ions that are the carriers of these charges. Therefore, calculations must consider divalent ions twice:

$$2\,(Ca^{2+}) + (H^+) = (OH^-) + (HCO_3^-) + 2\,(CO_3^{2-}) \qquad (9.11)$$

It should be noted that the parentheses (...) in this charge balance represent molar concentrations, since the chemical activities are not of importance here, instead the really existent amounts of the substances and their charges. Equation 9.11 describes in a simplified form the conditions in which the equilibrium state is reached starting from pure water. Only in this case all final concentrations produce charges equal to zero in the balance.

In an impure system, any initial concentration $(...)_i$ or initial activity $[...]_i$ may be present. In this context, the index 'i' stands for 'initial'. On the basis of these concentrations, those reached on attaining the final equilibrium state $(...)_f$ or $[...]_f$ will then have to be sought for. The index 'f' in this case stands for 'final'. The statement as to the charge balance made in Equation 9.11 is not accomplished by observing the total concentration of each reactant, but by the difference between 'initial' to 'final'. The generalized case described in Equation 9.12 resumes the condition of Equation 9.11 in which all initial concentrations are set to zero (pure water).

$$2\,(Ca^{2+})_f - 2\,(Ca^{2+})_i + (H^+)_f - (H^+)_i = (OH^-)_f - (OH^-)_i + (HCO_3^-)_f - (HCO_3^-)_i + 2\,(CO_3^{2-})_f - 2\,(CO_3^{2-})_i \qquad (9.12)$$

In a system following this description, the solution for all six variables (Ca^{2+}), (H^+), (OH^-), $(H_2CO_3^0)$, (HCO_3^-), (CO_3^{2-}) is sought for the condition of a final equilibrium state determined by the Equations 9.2, 9.4, 9.6, 9.8, 9.10, and 9.12. It should be noted that in Equations 9.2, 9.4, 9.6, 9.8, and 9.10 the activities written in brackets [...] are to be understood as final activities $[...]_f$, which are products of an activity coefficient and the single concentrations in equilibrium $(...)_f$ (cf. Eq. 15.2 in Sect. 15.1.1). For a system at infinite dilution, however, these activity coefficients are 1.0, and thus concentrations are (...) equal to activities [...].

The system of six non-linear equations with six unknown variables can be solved mathematically for $(H^+)_f$ by inserting the equations into each other until only constants, initial concentrations $(...)_i$, and pCO_2 describe the complete equation. This way of solving the problem leads to a cubic equation for which an analytical solution exists. In practice, however, this strategy is irrelevant, since such a set of equations cannot be analytically solved for other boundary conditions (e.g. a system which is closed with respect to CO_2, having no contact with the atmosphere) or if more constituents are included (e.g. complex species like $CaHCO_3^+{}_{aq}$ or $CaCO_3^0{}_{aq}$). In such a case, it must be solved by an iteration process, as will be described in the succeeding section. The application of spreadsheet calculation programs make such an iterative solution easy to find by pursuing the procedures below:

First, the concentration of $(H_2CO_3^0)_f$ is calculated on the basis of the given pCO_2 using Equation 9.2

Then, the pH-value of the equilibrium is estimated. For a first approximation, the pH-value derived from the 'initial' concentration of $(H^+)_i$ may be used. But any other pH-value, for instance pH 7, is permitted as well.

With this pH-value, the concentrations of $(H^+)_f$ and $(OH^-)_f$ are calculated using Equation 9.8.

Successively, $(HCO_3^-)_f$ and $(CO_3^-)_f$ are calculated using the Equations 9.4 and 9.6 and the values so far determined. The concentration of $(Ca^{2+})_f$ is obtained from Equation 9.12.

Now the saturation index $(SI_{calcite})$ can be calculated with Equation 9.10 (cf. Eq. 15.1 in Sect. 15.1.1). If the saturation index equals zero, then the estimation of the pH-value in equilibrium, as mentioned in step 2, has been correct, as well as all other equilibrium concentrations $(...)_f$ calculated in steps 3 and 4. If the saturation index $(SI_{calcite})$ is

not equal to zero with sufficient accuracy, the estimation for the pH in step 2 will have to be improved until the correct value is found.

Irrespective whether a solution to this system is found in the iterative manner described, or whether it is solved by finding an analytical solution of the cubic equation, the pH-value of the equilibrium is at all times determined by the partial pressure pCO_2 in the atmosphere. As it remains in contact with the solution, such a system is referred to as open to CO_2. It is characteristic of such systems that the reactions can cause the release of CO_2 into the atmosphere at any time and that CO_2 can be drawn from the atmosphere without directly affecting total atmospheric pCO_2.

9.3.2 Primary Reactions of the Calcite-Carbonate-Equilibrium without Atmospheric Contact

A system which is closed to CO_2 exists wherever the final calcite-carbonate-equilibrium is reached without any concurrent uptake or release of atmospheric CO_2 in its process. This implies that the Equations 9.1 and 9.2 are no longer valid. In their stead, a balance of various C-species is related to calcium. This balance maintains that the sum of C-species must equal the calcium concentration in solution, since both can enter the solution only by dissolution of calcite or aragonite:

$$(Ca^{2+}) = (H_2CO_3^0) + (HCO_3^-) + (CO_3^{2-}) \qquad (9.13)$$

Analogous to Equations 9.11 and 9.12, Equation 9.13 is only valid if the initial solution consists of pure water. In the normal case, in which the solution will already contain dissolved carbonate- and/or calcium ions, the difference between equilibrium concentrations $(...)_f$ and the initial concentrations $(...)_i$ needs to be regarded:

$$(Ca^{2+})_f - (Ca^{2+})_i = (H_2CO_3^0)_f - (H_2CO_3^0)_i + (HCO_3^-)_f - (HCO_3^-)_i + (CO_3^{2-})_f - (CO_3^{2-})_i \qquad (9.14)$$

The six Equations 9.4, 9.6, 9.8, 9.10, 9.12, and 9.14 must now be solved for the six variables (Ca^{2+}), (H^+), (OH^-), $(H_2CO_3^0)$, (HCO_3^-), (CO_3^{2-}). There is no analytical solution for this non-linear equation system. If there were one, it would be irrelevant because an iterative solution, similar to the one described in the previous section, would always be easier to handle and besides be more reliable. However, still independent of the method of mathematical solution is the fact that the equilibrium is exclusively determined by the carbonate concentration which the system previously contained and which is defined by the concentrations $(...)_i$. At this particular point, the amount of CO_2 would also have to be considered which is liberated into such a system, e.g. from the oxidation of organic matter. This amount would be simply added to the 'initial' concentrations and would influence the equilibrium in the same way as the pre-existing carbonate.

9.3.3 Secondary Reactions of the Calcite-Carbonate-Equilibrium in Seawater

In seawater, the differences between activities and concentrations must always be considered (cf. Sect. 15.1.1). The activity coefficients for monovalent ions in seawater assume a value around 0.75, for divalent ions this value usually lies around 0.2. In most cases of practical importance, the activity coefficients can be regarded with sufficient exactness as constants, since they are, over the whole range of ionic strengths in solution, predominately bound to the concentrations of sodium, chloride, and sulfate which are not directly involved in the calcite-carbonate-equilibrium. The proportion of ionic complexes in the overall calcium or carbonate content can mostly be considered with sufficient exactness as constant in the free water column of the ocean. Yet, this cannot be applied to pore water which frequently contains totally different concentrations and distributions of complex species due to diagenetic reactions.

Figure 9.4 shows the distribution of carbonate and calcium species in ocean water and in an anoxic pore water, calculated with the program PHREEQC (Parkhurst 1995). It is evident that about 10 % of total calcium is prevalent in the form of ionic complexes and 25 – 30 % of the total dissolved carbonate in different ionic complexes other than bicarbonate. These ionic complexes are not included in the equations of Sections 9.3.1 and 9.3.2. Accordingly, the omission of these complexes would lead to an erraneous calculation of the equilibrium. The inclusion of each complex shown in Figure 9.4 implies further additions to the system of equations, consisting in another concentration variable (the concentration of the complex) and a further equation (equilibrium of the complex concentration relative to the non-

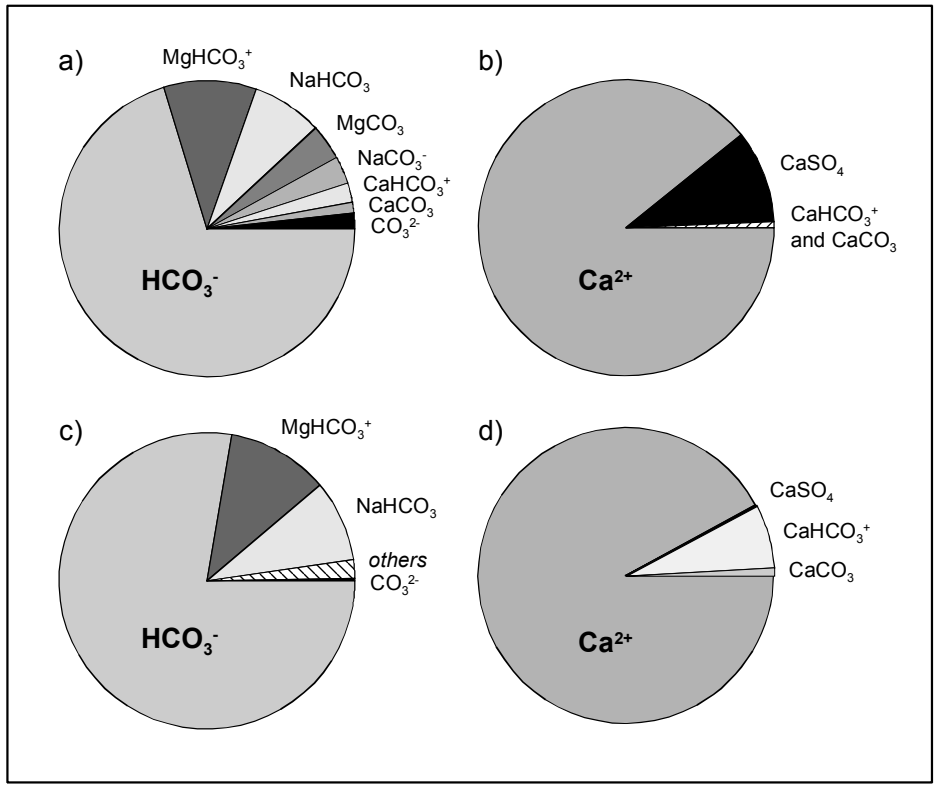

Fig. 9.4 Distribution of carbonate species (a and c) and calcium species (b and d) in seawater after Nordstrom et al. 1979 (a and b) and in an anoxic pore water (c and d). The pore water sample was extracted from the core previously shown in Figure 3.1 and was taken from a depth of 14.8 m below the sediment surface. The calculation of species distributions was performed with the program PHREEQC (Parkhurst 1995)

complexed ions). If only the ion complexes shown in Figure 9.4 are added, as there are ($MgHCO_3^+$), ($NaHCO_3^0$), ($MgCO_3^0$), ($NaCO_3^-$), ($CaHCO_3^+$), ($CaCO_3^0$), and ($CaSO_4^0$), the system would consequently be extended to 6+7=13 variable concentrations and just as many non-linear equations. Such a system of equations is solvable with the aid of an appropriate spread-sheet calculation program, however, that would be certainly not reasonable and would also be more laborious than using an equilibrium model of the PHREEQC type (Parkhurst 1995). Function and application of PHREEQC are described in Section 15.1 in more detail. In the following section, some calculation examples with regard to carbonate will be presented.

9.3.4 Examples for Calculation of the Calcite-Carbonate-Equilibrium in Ocean Waters

Here, exemplary results will be introduced which were obtained from model calculations of the calcite-carbonate-equilibrium under applied boundary conditions close to reality. To this end, the model PHREEQC (Parkhurst 1995) has been used. The chemical composition of the solution studied in these examples is based on analytical data published by Nordstrom et al. 1979 (cf. Table 15.1).

In the first example shown in Table 9.2, a warm (25°C) water from the ocean's surface (1 atm) has been modeled. In the zone near the equator, where this water sample had been taken, carbon dioxide partial pressures of 400 µatm (equivalent to a pCO_2 of 0.0004 atm or a log pCO_2 of -3.40) have been measured which is somewhat higher than the corresponding atmospheric value. This sample of ocean water thus displays a CO_2-gradient directed towards the atmosphere and therefore continually releases CO_2 into the atmosphere. This situation is accounted for in the model by pre-setting pCO_2 to 0.0004 atm as an open boundary condition with regard to CO_2. Accordingly, a state of supersaturation ensues equivalent to a $SI_{calcite}$ value of 0.77 or an $\Omega_{calcite}$ value of 5.9. Such a supersaturation state is, according to the

analytical evidence, obviously permanent by its nature, due to the processes in the surface-near ocean water and the fluxes across the interface ocean/atmosphere. The model results for a theoretical precipitation of calcite describing the state of calcite-carbonate-equilibrium ($SI_{calcite}$ = 0.0) are shown in the lower part of Table 9.2.

In the model calculation presented in Table 9.3, the constant of the solubility product of calcite was adjusted to temperature (6°C) and pressure (100 atm) relative to a depth of about 1000 m. Therefore, the pressure-corrected constant derived from the model SOLMINEQ (Kharaka et al. 1988) was entered into the database of the model PHREEQC, and the correction procedure for temperature integral to this model was used. Furthermore, an organic substance which also contained nitrogen and phosphorus in a C:N:P ratio of 106:16:1 (Redfield 1958), was decomposed down to a low residual concentration of dissolved oxygen. The calculation was then run under conditions closed to CO_2, i.e. concentrations of the previous example from Table 9.2 were regarded as 'initial'. The partial pressure pCO_2 in this case no longer represents a fixed boundary condition, but has now become a model output. The calcite-carbonate-equilibrium was kept at a constant state of supersaturation ($SI_{calcite}$ = 0.26) throughout all steps of the model calculation.

In the next example outlined in Table 9.4, a cold (2°C), surface-near (1 atm) ocean water sample has been modeled. In zones of high latitudes, where this water type occurs, a partial pressure of 280 µatm has been measured (equivalent to a pCO_2 of 0.00028 atm or a log pCO_2 of –3.55) which is somewhat lower than determined in the atmosphere. Here, the atmosphere displays a CO_2-gradient directed toward the ocean into which CO_2 is continually taken up.

This situation is accounted for in the model by pre-setting pCO_2 to 0.00028 atm, the boundary condition of a system open with regard to CO_2. Accord-

Table 9.2 Model calculation using the PHREEQC program (Parkhurst 1995) on a sample of warm surface water from the ocean near the equator. The lower part of the table shows the results for a theoretical ($SI_{calcite}$ = 0.0) precipitation of calcite.

Model of warm surface seawater		
input concentrations:		
dissolved constituents from Nordstrom et al. 1979, cf. Tabel 15.1		
boundary conditions:		
temperature	25 °C	
pCO_2	400 µatm	(i.e. log pCO_2 = -3.40)
log k calcite	-8,48	(at 25 °C and 1 atm pressure)
input situation without calcite-carbonate-equilibrium:		
pH	8,24	
sum of carbonate species (TIC)	2.17 mmol/l	
sum of calcium species	10.65 mmol/l	
$SI_{calcite}$	0,77	(i.e. $\Omega_{calcite}$ = 5.9)
reactions:		
calcite-carbonate-equilibrium constant at SI = 0.0		
PHREEQC model results:		
pH	7,50	
sum of carbonate species (TIC)	1.92 mmol/l	
sum of calcium species	10.40 mmol/l	
$SI_{calcite}$	0,00	(i.e. $\Omega_{calcite}$ = 1.0)

Table 9.3 Model calculation applying the computer program PHREEQC (Parkhurst 1995) to a sample of ocean water in a water depth of approximately 1000 m, near the equator. The constant of the solubility product for calcite is corrected for temperature and pressure. The decomposition of organic substance due to the presence of free oxygen in the water column has been included.

Model of low latitude seawater at 1000 m depth		
input concentrations:		
model calculation of warm surface seawater		
boundary conditions:		
temperature	6 °C	
log k calcite	-8.26	(at 6 °C and 100 atm pressure)
input situation without calcite-carbonate-equilibrium:		
pH	8.08	
sum of carbonate species (TIC)	2.26 mmol/l	
sum of calcium species	10.61 mmol/l	
$Si_{calcite}$	0.26	(i.e. $\Omega_{calcite}$ = 1.8)
reactions:		
$(CH_2O)_{106}(NH_3)_{16}(H_3PO_4)$ reacts with dissolved O_2		
calcite supersaturation constant at SI = 0.26		
PHREEQC model results:		
pH	8.01	
sum of carbonate species (TIC)	2.60 mmol/l	
sum of calcium species	10.79 mmol/l	
$Si_{calcite}$	0.26	(i.e. $\Omega_{calcite}$ = 1.8)

ingly, a state of supersaturation ensues equivalent to a $SI_{calcite}$ value of 0.43 or an $\Omega_{calcite}$ value of 2.7. As a theoretical example (lower part of Table 9.4) for the modeling in this case a constant state of supersaturation according to a $SI_{calcite}$ value of 0.50 or an $\Omega_{calcite}$ value of 3.2 was calculated.[1]

In the calculated model summarized in Table 9.5, the equilibrium constants for calcite was adjusted to temperature (2°C) and pressure (600 atm) of a water depth of about 6000 m. In this example as well, the pressure-corrected constant derived from the model SOLMINEQ (Kharaka et al. 1988) was entered into the database of the model PHREEQC, and the correction procedure for temperature of this model was used. Calculation was run under the boundary conditions of a system closed with regard to CO_2, i.e. the concentrations of the previous example in Table 9.4 were regarded as 'initial'. The partial pressure pCO_2 is not a fixed boundary condition of an open system, and it did not change as in the example shown in Table 9.3, since no reactions were determined. A comparable decomposition of organic matter as in Table 9.3 was thus excluded from this example. After pressure-correction, the saturation index of calcite documents an undersaturation displaying a value of –0.16 (equivalent to a $\Omega_{calcite}$ value of 0.69). In the case of an additional decomposition of organic matter, this undersaturation of calcite is likely to increase further. Such a reaction could be in fact applicable to deep-sea waters of pelagic deep ocean areas.

[1] $\Omega_{calcite}$ is still in use in chemical oceanography for describing the state of saturation. It corresponds to the saturation index without the logarithm, hence: log $\Omega_{calcite} = SI_{calcite}$. However, the SI value is more useful, since the same amounts of undersaturation and supersaturation respectively display the same SI values, only distinguished by different signs (+) for supersaturation and (-) for undersaturation. A SI value of zero describes the state of saturation.

Table 9.4 Model calculation applying the computer program PHREEQC (Parkhurst 1995) to a sample of cold surface water of the ocean from higher latitudes. The constant of the solubility product for calcite is accordingly corrected for temperature.

Model of cold surface seawater

input concentrations:

dissolved constituents from Nordstrom et al. 1979, cf. Tabel 15.1

boundary conditions:

temperature	2 °C	
pCO_2	280 µatm	(i.e. log pCO_2 = -3.55)
log k calcite	-8,34	(at 2 °C and 1 atm pressure)

input situation without calcite-carbonate-equilibrium:

pH	8,23	
sum of carbonate species (TIC)	2.28 mmol/l	
sum of calcium species	10.63 mmol/l	
$SI_{calcite}$	0,43	(i.e. $\Omega_{calcite}$ = 2.7)

reactions:

calcite supersaturation constant at SI = 0.50

PHREEQC model results:

pH	8,30	
sum of carbonate species (TIC)	2.30 mmol/l	
sum of calcium species	10.65 mmol/l	
$SI_{calcite}$	0,50	(i.e. $\Omega_{calcite}$ = 3.2)

9.4 Carbonate Reservoir Sizes and Fluxes between Particulate and Dissolved Reservoirs

Present-day production of calcium carbonate in the pelagic ocean is calculated to be in the order of 6 to 9 billion tons (bt) per year ($60\text{-}90 \cdot 10^{12}$ mol yr^{-1}), from which about 1.1 to 2 bt (11 to $20 \cdot 10^{12}$ mol yr^{-1}) accumulate in sediments (Tables 9.1 and 9.6). Together with the accumulation in shallow waters of $14.5 \cdot 10^{12}$ mol yr^{-1} (Table 9.1, Fig. 9.5), the total carbonate accumulation in the world ocean amounts to 3.5 bt per year. This latter number is twice as much calcium as is brought into the ocean by rivers and hydrothermal activity (1.6 bt, Wollast 1994). Wollast (1994) and Milliman and Droxler (1996) therefore consider the carbonate system of the modern ocean to be in non-steady state conditions, because production is not equal to the input of Ca^{2+} and HCO_3^- by rivers and hydrothermal vents (Fig. 9.5). Consequently, the marine carbonate system is at a stage of imbalance, or the output controlled by calcite sedimentation or input conveiled by dissolution has been overestimated or underestimated, respectively. On the other hand, one or more input sources may have been not detected so far. Published calcium carbonate budgets vary strongly, because the various authors have used different data sets and made different assumptions with respect to the production and accumulation of carbonates (e.g. Table 9.6), as well as for the sources of dissolved calcium and carbonate in marine waters (see summaries in Milliman 1993; Milliman and Droxler 1996; Wollast 1994).

Table 9.5 Model calculation using the computer program PHREEQC (Parkhurst 1995) on deep-sea waters of the ocean. The constant of the solubility product for calcite is accordingly corrected for temperature and pressure. A comparable decomposition of organic matter as contained in Table 9.3 was excluded in this example.

Model of seawater at 6000 m depth

input concentrations:

model calculation of cold surface seawater

boundary conditions:

temperature	2 °C	
pCO_2	280 µatm	(i.e. log pCO_2 = -3.55)
log k calcite	-7.75	(at 2 °C and 600 atm pressure)

input situation without calcite-carbonate-equilibrium:

pH	8.23	
sum of carbonate species (TIC)	2.28 mmol/l	
sum of calcium species	10.63 mmol/l	
$Si_{calcite}$	0.43	(i.e. $\Omega_{calcite}$ = 2.7)

no reactions, but pressure changed to 600 atm

PHREEQC model results:

pH	8.23	
sum of carbonate species (TIC)	2.28 mmol/l	
sum of calcium species	10.63 mmol/l	
$Si_{calcite}$	-0.16	(i.e. $\Omega_{calcite}$ = 0.7)

9.4.1 Production *Versus* Dissolution of Pelagic Carbonates

This chapter summarizes the most recent compilations of carbonate reservoir size in the ocean and sediments, as well as the particulate and dissolved fluxes (Fig. 9.5) provided by the above mentioned authors. Coral reefs are probably the best documented shallow-water carbonate environment. Carbonate production on reef flats range as high as 10.000 g $CaCO_3$ $m^{-2}yr^{-1}$, with a global mean of about 1800 g $CaCO_3$ $m^{-2}yr^{-1}$. Totally this amounts to $24.5 \cdot 10^{12}$ mol yr^{-1} (Table 9.1) from which $14.5 \cdot 10^{12}$ mol yr^{-1} accumulate and $10 \cdot 10^{12}$ mol yr^{-1} are transported to the deep-sea either by particulate or dissolved export. One of the most uncertain numbers in all these budget calculations are the estimates of the global carbonate production in the open ocean. Milliman's (1993) estimate was only about $24 \cdot 10^{12}$ mol yr^{-1}, based on carbonate flux rates at about 1000 m water depth, measured by long-term time series of sediment trap moorings, which is approximately 8 g $CaCO_3$ $m^{-2}yr^{-1}$ accounting for a global flux rate of particulate pelagic carbonate to be in the range of $24 \cdot 10^{12}$ mol yr^{-1}. However, as discussed in Wollast (1994), in order to produce the measured water column profiles of total inorganic carbon and carbonate alkalinity (Fig. 9.3) a much higher surface ocean carbonate production is required. Thus estimates reported more recently are in the order of 60 to $90 \cdot 10^{12}$ mol yr^{-1} (Table 9.6). The discrepancy between the very high global production rates and measured fluxes obtained in sediment traps then can only be explained if one accepts that a substantial portion (30 to 50 %) of carbonate produced in the pelagic

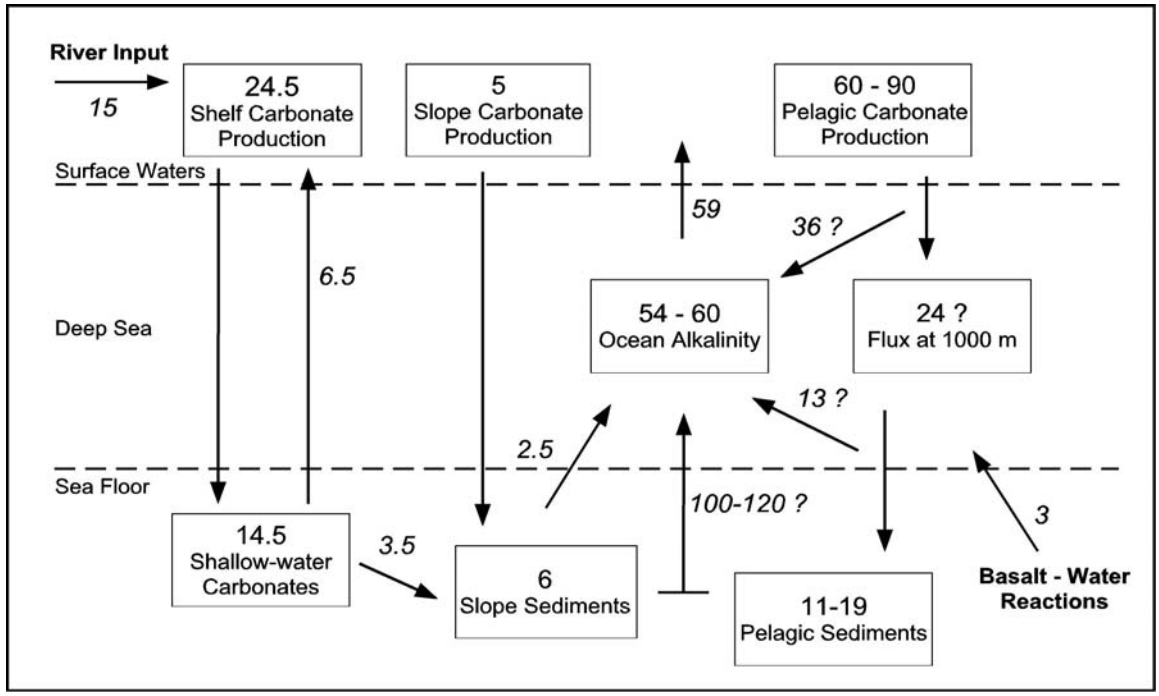

Fig. 9.5 Production, accumulation and fluxes of marine inorganic carbon (in x 10^{12} mol yr^{-1}) in the modern ocean, summarizing production, accumulation, and fluxes of particulate inorganic carbon, as well as carbonate dissolution rates as given in Table 9.1 (modified after Milliman and Droxler 1996, Wollast 1994).

ocean is already dissolved in the upper 1000 m of the ocean. On the other hand, if calcite dissolution above lysocline depths due to benthic respiration of organic matter (e.g. Emerson and Bender 1981; see also discussion and references below) is much higher as previously thought, then the fraction of pelagic carbonate production which reaches the sea floor prior to benthic respiration maybe in the order of 50 to 70 % and not only about 20 % as given in Table 9.6 for the more recent budget estimates. According to Archer (1996b) 20-30 % of the carbonate flux to the sea floor finally escapes dissolution. If this is correct, it would require a much less total carbonate production in the surface ocean (in the order of the estimate of Milliman (1993); see Table 9.6), to maintain measured water column profiles of alkalinity and total dissolved inorganic carbon, as well as $11 \cdot 10^{12}$ mol yr^{-1} of pelagic carbonate sedimentation. To solve the problem whether high

Table 9.6 Comparison of carbonate rain, accumulation and dissolution estimates for the pelagic ocean (all values in 10^{12} mol yr^{-1}).

Author	Pelagic Production	Burial	Dissolution	Burial fraction of Production
Milliman (1993)	24	11	12	47%
Milliman & Droxler (1996)	60	11	13 36 already at 1000 m, Table 9.1, w ith about 6 from sediments above the hydrogr. lysocline (Hensen et al. 2003).	18%
Wollast (1994)	65	11	54	18%
Archer (1994) (as cited in Archer 1996b, Fig. 12)	86	19	67	22%
Hensen et al. (2003)			22-81	

values of alkalinity and total dissolved inorganic carbon in intermediate and deep waters are the result of dissolving calcite particles settling through the water column, or of sedimentary dissolution above the lysocline, would require better knowledge of the total amount of calcite production in the surface ocean and of the dissolution rates in the sediment. While the first is very difficult to measure, the second may be reached by improving data sets of inorganic carbon flux rates from the sediment to ocean at intermediate and deep water levels. The next Section 9.4.2. describes the approach of estimating the fluxes of total carbon and inorganic carbon resulting from calcite dissolution in more detail.

9.4.2 Inorganic and Organic Carbon Release from Deep Sea Sediments

Although only a small fraction of carbon arriving at the seafloor is finally buried, over geological time scales deep sea sediments have formed the largest reservoir of carbon on earth mainly consisting of biogenic carbonates (~50 Mio. Gt) and organic detritus (~12 Mio. Gt; i.e. de Baar & Suess, 1993). This huge storage potential of marine carbonates is a major factor for maintaining reasonably low atmospheric CO_2-levels in earth history. However, the ratio of accumulation versus recycling of carbon at the seafloor reflects a dynamic equilibrium depending on various external forcing factors. Hence, the question for the "how much is being recycled" is an important issue, but quite difficult to explore.

Diagenetic mineralization and dissolution processes in deep sea sediments have been recognized as important control factors and numerous efforts have been made to estimate the contribution by benthic reflux to the ocean budget. The diagenetic reactions are most intense at the sediment-water interface where the most labile components become rapidly mineralized. Hence, this is the place where the determination between burial and recycling is made. The driving forces of carbon release from the sediments are the degradation of organic matter and the dissolution of calcium carbonate, which are in turn dependent on the supply by the remnants of biological production in the surface waters. However, the dissolution of calcium carbonate in deep-sea sediments is controlled by two major factors, the degree of undersaturation of the deep ocean waters with respect to calcite and aragonite, and the reaction with carbon dioxide from respiration processes. Two of the key parameters are thus, the "rain ratio" (C_{CaCO3} /C_{POC}) of the sinking material and the water depth of final deposition, above or below the CO_3^{2-} saturation horizon (lysocline). Because the solubility of calcium carbonate increases with increasing pressure, the ocean is usually super-saturated at shallow to intermediate depths and undersaturated in the deep basins.

Another important effect, which has been outlined in Chapter 6.2, is the ageing, or better the respiratory enrichment in CO_2 of the deep waters along the flow path from the North Atlantic to the North Pacific causing large differences in saturation state above the seafloor in the Atlantic and the Pacific (Fig. 9.6).

While calcite dissolution below saturation horizons in the water column can be described by the equations reported in section 9.3.2., dissolution due to CO_2 release from organic carbon respiration is expressed by the following equations:

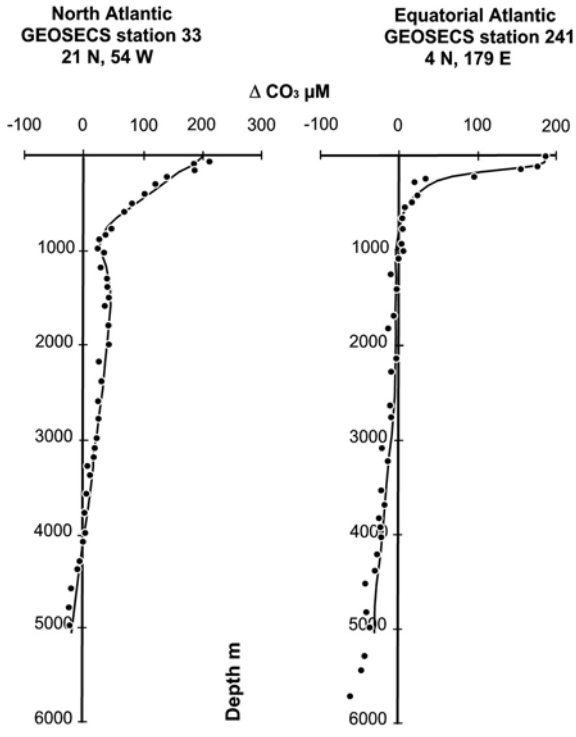

Fig. 9.6 ΔCO_3^{2-} (giving the difference between the saturation concentration of CO_3^{2-} and the ambient concentration of CO_3^{2-} at a specific depth) based on GEOSECS-data (Takahashi et al., 1980) of two locations in the Atlantic and the Pacific ocean. The intersection of the data points with the 0 µM line denotes the position of the lysocline (from Archer, 1996).

$$(CH_2O)_{106}(NH_3)_{16}(H_3PO_4) + 138\ O_2 \rightarrow$$
$$106\ HCO_3^- + 16\ NO_3^- + HPO_4^{2-} + 16\ H_2O + \mathbf{124\ H^+} \quad (9.15)$$

$$124\ CaCO_3 + \mathbf{124\ H^+} \rightarrow 124\ HCO_3^- + 124\ Ca^{2+} \quad (9.16)$$

where organic matter with Redfield C:N:P ratio is oxidized and the produced acid is neutralized by sedimentary calcium carbonate.

Carbonate dissolution induced by metabolic processes in deep-sea sediments has been neglected for a long time. Emerson and Bender (1981) were about the first who explicitly stated that the degradation of organic matter may significantly drive calcite dissolution, and hence, affect the preservation of calcium carbonate in deep-sea sediments even above the lysocline. A number of subsequent studies has identified this problem and generally focused on the differentiation between calcium carbonate dissolution by undersaturation of bottom waters and organic matter remineralization. These studies specifically considered the dissolution kinetics of calcium carbonate in deep-sea sediments (i.e. Berelson et al. 1990; Berelson et al. 1994; Hales and Emerson 1996 and 1997a; Jahnke et al. 1994 and 1997; Martin and Sayles 1996; Wenzhöfer et al. 2001). It is very important to understand whether the dissolution of calcium carbonate is driven by one or the other process in order to correctly interpret the accumulation of calcium carbonate in sediments over time. For example, calcium carbonate preservation at a given site may be reduced by stronger bottom water undersaturation or the decrease of the rain ratio by accelerating the metabolic CO_2 release in the sediments. Archer and Maier-Reimer (1994) demonstrated that a shift to higher rain ratios could explain both, reduced pCO_2-levels during the last glacial and sedimentary calcium carbonate concentrations in deep-sea sediments. The calcite dissolution by oxic respiration of organic matter might therefore be able to mask effects of changes in carbonate productivity and deep-water chemistry in the sedimentary carbonate record (Martin and Sayles, 1996).

For a long time it was not possible to calculate the benthic total carbon dioxide or alkalinity flux because of artifacts introduced by decompression processes during core recovery. Moreover there was no established method for predicting a true concentration profile or benthic flux (Murray et al. 1980; Emerson and Bender 1981; Emerson et al. 1980; Emerson et al. 1982). What happens during recovery of cores from some thousand meters of water depth is that the solubility of CO_2 in the pore water is increasingly reduced due to decompression and warming. Probably, dependent on the calcium carbonate content of the sediment providing nucleation sites, calcium carbonate is then precipitated from the pore water on the way through the water column. Calculation of the diffusive alkalinity flux across the sediment-water interface from such cores may thus, largely underestimate the real flux or even suggest a flux directed into the sediments (cf. chapter 6).

In the last decade, however, in-situ techniques have been developed to overcome these problems. Profiling lander systems were deployed to record the pore water microprofiles of oxygen, pH and pCO_2, and Ca whereas benthic chambers were deployed to measure solute fluxes across the sediment-water interface directly. Very often, reactive-transport models are used to explain the interrelation between measured microprofiles, to predict overall calcite dissolution rates by defining the dissolution rate constants, and to distinguish between dissolution driven by organic matter oxidation and by the undersaturation of the bottom water.

In most of recently published studies, the calcium carbonate dissolution in seawater and in pore water of surface sediments is assumed to follow a kinetic process that can be described by the equation (Morse 1978; Keir 1980):

$$R_d = k_d\ (1 - \Omega)^n \quad (9.17)$$

$$\Omega = \frac{[Ca^{2+}][CO_3^{2-}]}{k} \quad (9.18a)$$

$$SI = \log \frac{[Ca^{2+}][CO_3^{2-}]}{k} \quad (9.18b)$$

where R_d is the calcite dissolution rate, k_d is the calcite dissolution rate constant, and Ω or SI describe the degree of saturation (ion activity product divided by k), and k the solubility constant of the calcium carbonate species in question. Mostly, k´ is used instead of k, which is defined as the apparent solubility constant and is

related to concentrations instead of activities. Compilations of apparent solubility constants are available e.g. by Mehrbach et al. (1973). In several studies, a further dependence of R_d on the calcium carbonate content (respectively the surface area) in the sediment is considered. (for a more detailed overview of this subject see Zeebe and Wolf-Gladrow 2000).

The most extensively used reaction order for modeling calcite dissolution is 4.5 and 4.2 for aragonite (as suggested by Keir 1980). A more extensive re-evaluation of this topic has been provided by Cai et al. (1995). However, the discussion concerning the "correct" reaction order still continues. The values of k_d reported so far range over several orders of magnitude from 0.005-0.16 % d^{-1} (Berelson et al. 1994; Hales and Emerson 1996, 1997a) up to laboratory values of 10-1000 % d^{-1} (Keir 1980, 1983)[2]. The reason for this huge discrepancy is not clearly known. Important and regionally variable factors, however, may be the grain size and thus the surface area of calcium carbonate crystals in the sediments or adsorbed coatings like phosphate ions protecting calcium carbonate grains from corrosive pore waters (Jahnke et al. 1994; Hales and Emerson 1997a). In contrast, Hales and Emerson (1997b) found evidence that *in-situ* pH measurements in pore waters of calcite rich deep-sea sediments are more consistent with a first-order instead of 4.5th order dependence. Applied to their data, they re-wrote Equation 9.17 to

$$R_d = 38\ (1- \Omega)^1 \qquad (9.19)$$

In contrast, the study of calcite dissolution kinetics in $CaCO_3$-poor sedi-ments of the equatorial Atlantic, Adler et al. (2001) again favored higher reaction orders. In this sense, the observed dissolution rate constants are highly variable, which seems to be mainly dependent on differences in the physical (e.g. surface area) and chemical properties (high/low Mg-calcite) of the calcite mineral phase.

It is also important to consider where in the sediment dissolution occurs. Metabolically produced CO_2 released immediately at the sediment-water interface is probably much less effective for carbonate dissolution than in deeper sediment strata, because neutralization with bottom water CO_3^{2-} might occur instead of dissolution. If the particulate organic matter is more rapidly mixed down, i.e. by bioturbation, and oxidized in deeper sediment strata, the CO_2 released into the pore waters can probably more effectively dissolve carbonates (Martin and Sayles 1996).

It is generally reported that dissolution at and above the saturation horizon is solely attributed to the oxidation of organic matter. The importance of oxidation-related dissolution decreases with increasing undersaturation of the bottom water, however, the efficiency by which C_{org} oxidation drives $CaCO_3$ dissolution increases with increasing undersaturation of the bottom water (Martin and Sayles 1996). In the same sense, Berelson et al. (1994) suggested that the undersaturation of the bottom water is more important for better soluble calcite phases (high k-values), whereas for more resistant calcite phases (low k-values), the rain of C_{org} to the seafloor, and thus mineralization, becomes the driving force for calcite dissolution (Fig. 9.7). This can be understood as an alteration process, where dissolution starts at the sediment-water interface, right after deposition of the calcite phase, and becomes more resistant to dissolution during burial. In the zone of oxic respiration the removal of organic coatings around calcite grains might also play an important role since they help to expose larger surface areas to the pore water, thus triggering dissolution processes.

In summary, a closer evaluation of Fig. 9.7 reveals:

(1) It is obvious that for low oxygen fluxes the relative importance of bottom water undersaturation is the driving force for $CaCO_3$ dissolution, meaning that the y-axis intercept is exceptionally determined by k_d and Ω.

(2) It is implicit from Eq. 9.17 that a higher degree of undersaturation increases the differences of dissolution fluxes between the chosen values of k_d (distance between hatched and solid lines).

(3) Higher oxygen fluxes (higher amount of metabolically released CO_2) are obviously more efficient in carbonate dissolution when bottom waters are stronger undersaturated (lower Ω).

[2] The unit % d^{-1} originates from experimental studies (e.g. Morse 1978; Keir 1980) and is used in most studies dealing with carbonate dissolution in marine sediments. The use is, however, not always consistent regarding the units of the dissolution rate and the parameters used in the equation and should, therefore, generally be evaluated with caution.

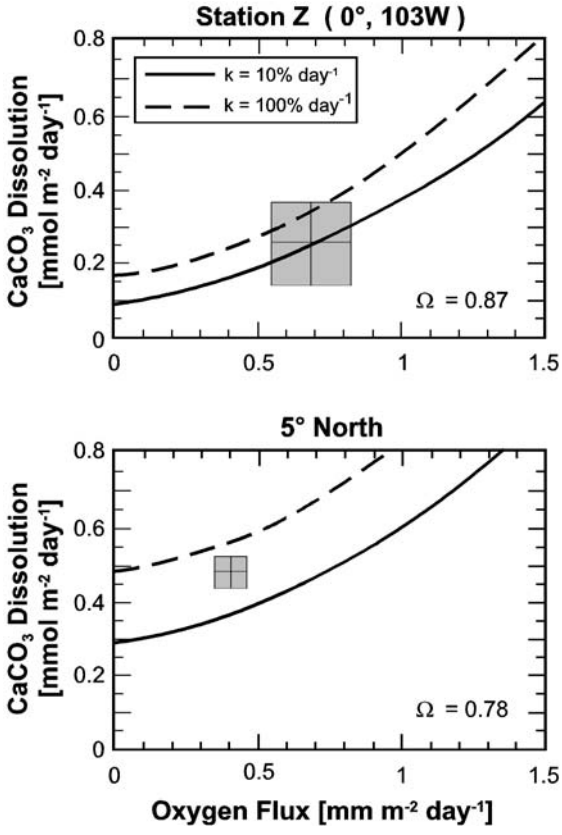

Fig. 9.7 Model results of calcium carbonate dissolution rates as a function of oxygen uptake rates and degree of saturation with different values of k_d from Berelson et al. (1994). The boxes represent averaged benthic lander fluxes for each station (see text for explanation).

(4) For high oxygen fluxes the model predicts a ratio of calcite dissolution and oxygen flux of 0.85 which is close to the stoichiometrical ratio in Eq. 9.15.

More recently *in situ* microsensor measurements of O_2, pH, pCO_2, and Ca could be obtained from the upper continental slope off Gabon (Wenzhöfer et al. 2001; Adler et al. 2001; Pfeifer et al. 2002), which, to date, provide one of the most complete sets of non-corrupted pore water data from deep-sea sediments. The bottom water at a water depth of about 1300 m is slightly oversaturated with respect to calcite (Ω = 1.07 and 1.10, Adler et al. 2001), thus, dissolution must exclusively be mediated by metabolically produced CO_2. For the first time, *in situ* measurements of all parameters describing the carbon dioxide system, combined with O_2 microprofiles, permitted the quantification of the amount of C_{org} mineralization relative to $CaCO_3$ dissolution. These were completed by a number of *ex situ* parameters. The numerical model CoTReM was applied to investigate the depth dependent effects of respiration and redox processes related to $CaCO_3$ dissolution (Pfeifer et al. 2002; cf. Fig. 15.16 in chapter 15). Interestingly, if calculated until a steady-state situation is reached, the model-derived calcite dissolution and precipitation rates produce an almost perfect fit to the measured $CaCO_3$ profile in the sediment (Fig. 9.8), which suggests that ~90 % of the $CaCO_3$ flux to the sea floor is redissolved in the sediment.

It is important to note that calcite dissolution is exceptionally driven by oxic respiration (Eq. 9.15, 9.16) and re-oxidation of reduced species like HS^-. Subsequent degradation processes like the reduction of iron oxides (Eq. 9.20) may even have the opposite effect leading to the precipitation of calcium carbonate. Sulfate reduction (Eq. 9.21) is less efficient than oxic respiration, which is related to at least three important facts, which are (1) lower overall reaction rates, (2) a lower potential of acid production, and (3) a higher buffer capacity due to rising alkalinity levels in the pore water with increasing sediment depth. Because manganese and iron reduction are only of minor importance in terms of total mineralization (cf. Chapter 6), significant amounts of carbonate precipitation are usually not observed (Raiswell and Fisher 2004). A major process driving carbonate precipitation in sediments is the anaerobic oxidation of methane (AOM; see Chapter 8). However, the formation of visible or massive authigenic carbonates (crusts and chimneys) is restricted to cold seep environments, where methane-enriched fluids are advected at sufficient rates (Luff and Wallmann 2003; Luff et al. 2004).

$$(CH_2O)_{106}(NH_3)_{16}H_3PO_4 + 424Fe(OH)_3 \rightarrow 106HCO_3^- + 16NH_4^+ + HPO_4^{2-} + 424Fe^{2+} + 304H_2O + \mathbf{756}\boldsymbol{OH}^- \quad (9.20)$$

$$(CH_2O)_{106}(NH_3)_{16}H_3PO_4 + 53SO_4^{2-} \rightarrow 106HCO_3^- + 16NH_4^+ + HPO_4^{2-} + 53HS^- + \mathbf{39}\boldsymbol{H}^+ \quad (9.21)$$

In the study of Pfeifer et al. (2002) calcite dissolution fluxes have been quantified in two different ways: (1) by calculating the Ca^{2+}-gradient from the sediment into the bottom water of the Ca-microprofile (Wenzhöfer et al. 2001b) and (2) by the model derived dissolution rates (Fig. 9.8). Following the model approach, Ca-fluxes resulted

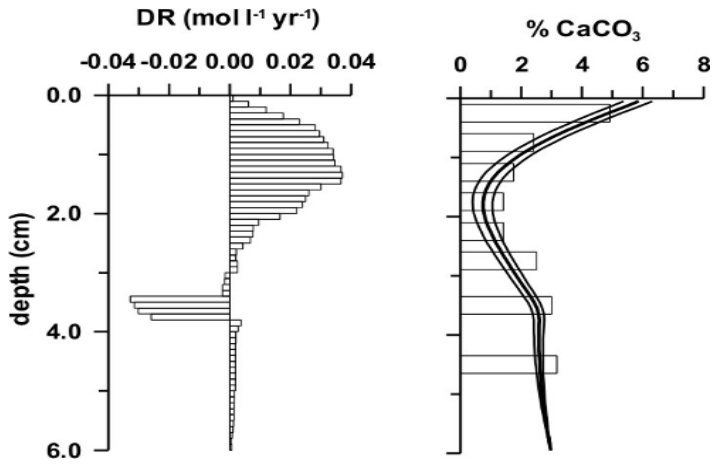

Fig. 9.8 Measured and simulated pore water profiles at station GeoB 4906 and corresponding rates of primary and secondary redox processes. (b) Corresponding calcite dissolution and precipitation rates and the resulting steady-state distribution of sedimentary $CaCO_3$ for input fluxes of 40, 42, and 44 g $m^{-2}yr^{-1}$, respectively, compared to measured concentrations (bars) (after Pfeifer et al. 2002).

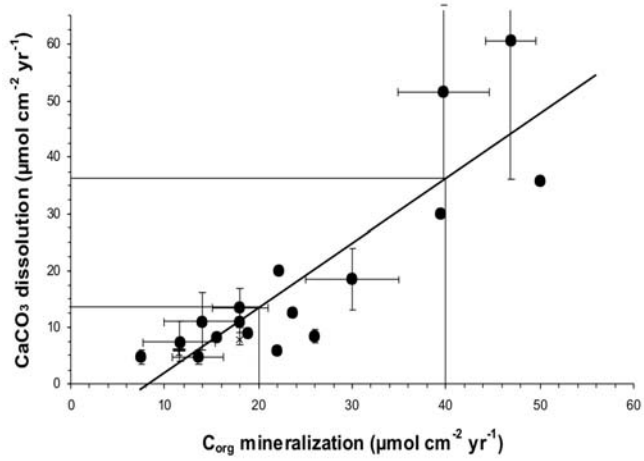

Fig. 9.9 Compilation of literature-derived $CaCO_3$ dissolution fluxes vs. C_{org} mineralization rates from deep-sea sediments (after Pfeifer et al. 2002). Equation 9.22 implies that there exists a considerable threshold of mineralization, which has to be exceeded before $CaCO_3$ dissolution is initiated. The increasing proportion of $CaCO_3$ dissolution with increasing mineralization is indicated by the vertical and horizontal lines.

in 35.8 µmol cm^{-2} yr^{-1} at site GeoB 4906 and 33 µmol cm^{-2} yr^{-1} at site GeoB 4909, whereas calcite dissolution fluxes calculated directly from Ca-microprofiles are distinctively lower with 20.1 and 21.2 µmol cm^{-2} yr^{-1}, respectively (attributed to scattering data and inconsistencies in the measured profiles).

Combining these results with existing data on calcite dissolution fluxes and C_{org} mineralization rates from deep-sea sediments located above the saturation horizon and slightly below ($\Omega \sim 0.8$; Fig. 9.9) results in a good correlation, which has been used to derive a general empirical formulation relating calcite dissolution and C_{org} mineralization (Pfeifer et al. 2002):

$$DR_{CaCO_3} = 1.1 \cdot MR_{C_{org}} - 9.3 \qquad (9.22)$$

where DR_{CaCO3} is the calcite dissolution flux and MR_{Corg} is the C_{org} mineralization rate (both in µmol cm^{-2} yr^{-1}).

Using Eq. 9.19, Hensen et al. (2003) calculated an estimate of the global calcite dissolution flux above the hydrographic lysocline by application of a GIS-system (Fig. 9.10). To define the position of the hydrographic lysocline, the gridded global

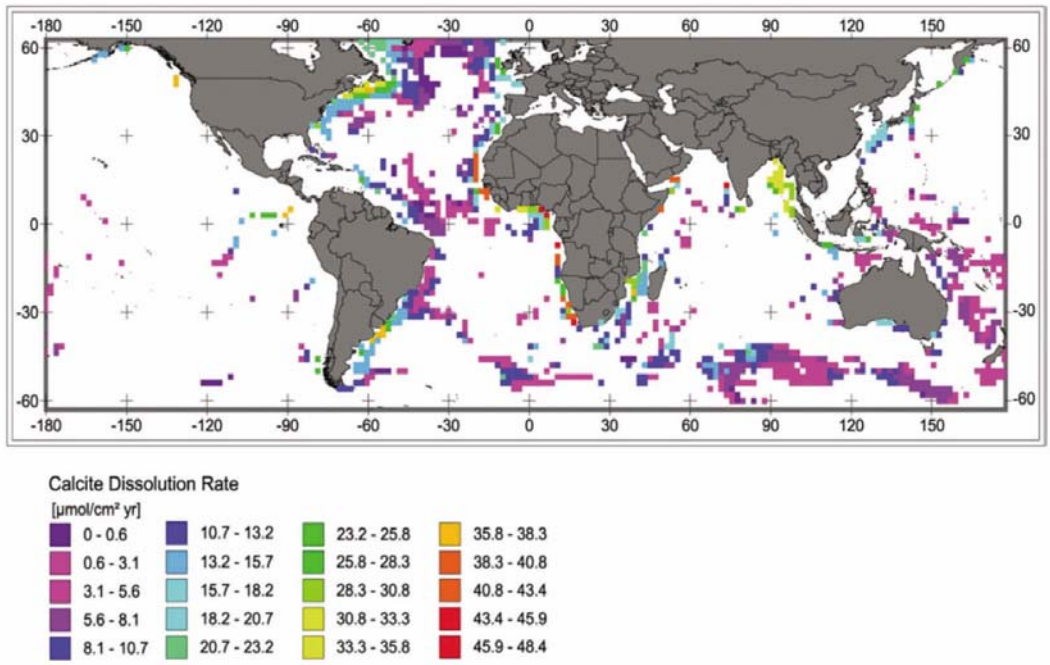

Fig. 9.10 Map showing the global distribution of supralysoclinal calcite dissolution by applying Equation 9.19, based on global grids of bottom water "CO_3^{2-} (Archer 1996a) and oxygen consumption rates (Jahnke 1996) (from Hensen et al. 2003).

field of bottom water ΔCO_3^{2-} data (Archer 1996a) has been used and C_{org}-mineralization rates from the grid of oxygen consumption rates after Jahnke (1996) have been calculated, assuming a Redfield ratio of decomposed organic material. The global sea floor area above the lysocline was estimated to about $7.4 \cdot 10^7$ km^2 (corresponding to ~20 % of the total ocean area) and the dissolution flux sums up to about $5.7 \cdot 10^{12}$ mol $CaCO_3$.

Taking into account more recent estimates for the global oxygen demand of the seafloor (i.e. Wenzhöfer and Glud 2002) respiratory driven calcite dissolution can be expected to be 50 % higher in total. Compared to Archer's study in 1996 (see Table 9.7), this would add ~10-20 % to the total estimate.

In comparison with the study of Archer (1996b), the estimate of Milliman et al. (1999) clearly underestimates the total benthic $CaCO_3$-dissolution. Actually, simply using the Archer-flux would help to resolve a long lasting debate and balances – more or less – the overall budget shown in Fig 9.5.

Milliman et al. (1999) postulated an enormous loss of $CaCO_3$ in the upper water column for, to date, unknown reasons. Jansen et al. (2002) used a numerical model in order to investigate and predict, whether such a loss could be attributed to respiration-driven dissolution of skeletal material in microenvironments of sinking detritus. Although the efficiency of this process is largely dependent on the sinking velocity and the size of the sinking spheres or particles, these authors could show that this pathway of carbonate dissolution does not account significantly to the overall loss as observed by Milliman et al. (1999).

Applying Equation 9.22 for the total sea floor area should give a reasonable estimate for the metabolically induced $CaCO_3$-dissolution on a global scale, even though this must be less than the total dissolution flux from respiration and bottom water undersaturation. The application C_{org}-mineralization rates derived from various estimates of the global oxygen consumption in deep-sea sediments (Jahnke 1996; Christensen 2000; Wenzhöfer and Glud 2002; Seiter et al. 2005) results in global fluxes of $CaCO_3$-dissolution between $14.8 \cdot 10^{12}$ and $47.2 \cdot 10^{12}$ mol yr^{-1}. These comparatively low efficiencies of $CaCO_3$ dissolution in combination with a wide range of estimates are the result of the significant threshold value of about 8 µmol cm^{-2} yr^{-1} before $CaCO_3$ dissolution is initiated (Fig. 9.9). More precisely, the low average mineralization rates of 12.9 µmol cm^{-2} yr^{-1} as derived from the lowest estimate by Jahnke (1996) would proportionally be much less

efficient in terms of $CaCO_3$ dissolution than higher estimates of up to 31.6 cm^{-2} yr^{-1} (derived from Wenzhöfer & Glud 2002). This is in contradiction with studies of Reimers et al. (1992) and Hammond et al. (1996) who predict that mineralization and carbonate dissolution contribute about one half each to the total dissolved carbon (DIC) or alkalinity fluxes. This 1:1 relationship obviously proves true only for higher mineralization rates (Fig. 9.9).

Nevertheless, in combination with Archer's results from the non-respiratory dissolution runs (7-34 · 10^{12} mol yr^{-1}) the global $CaCO_3$-dissolution flux may range between 22 to 81 · 10^{12} mol yr^{-1} (Hensen et al. 2003). On the one hand, it confirms Archer's results based on a number of newly obtained *in situ* measurements from different deep-sea locations, and, on the other hand, it suggests that calcite dissolution fluxes to the seafloor that even Archer's maximum estimation of 54 · 10^{12} mol yr^{-1} might be even an underestimation, if higher benthic mineralization rates as derived from Christensen (2000) and Wenzhöfer and Glud (2002) prove true (compare with Milliman's estimate).

A compilation of recent data on carbon re-flux from deep-sea sediments is provided in Table 9.7. Four flux categories are given in Table 9.7: The CO_2 produced due to oxic respiration, calcite dissolution, the alkalinity as a sum parameter for calcium carbonate dissolution and CO_2 from oxic respiration, and, hitherto neglected in the discussion, the dissolved organic carbon (DOC).

It is very interesting to note that many of the more recently obtained calculations agree very much with those of Berelson et al. (1994) who calculated the benthic alkalinity input to the deep ocean for the Pacific and the Indo-Pacific (Table 9.7). They suggested that most of the carbonate dissolution in the deep ocean (Fig. 9.5) occurs within the sediments (85 %). The extension of their results from Pacific and Indian Ocean to the Atlantic Ocean leading to 120 · 10^{12} mol yr^{-1} of global dissolved carbon fluxes from sediments may, however, be critical because of the completely different deep-water conditions in the Indo-Pacific and the Atlantic. Deep ocean waters in the Indian and Pacific Oceans are known to be much older and depleted in CO_3^{2-} implying that a much higher proportion of calcite dissolution contributes to the total alkalinity input there. However, despite this problem of different bottom-

Table 9.7 Carbon fluxes from deep-sea sediments (below 1000 m water depth) in 10^{12} mol yr^{1} estimated by using different parameters. Global estimations of regional data compilations are made by multiplication with surface area factors.

Parameter	Area	Flux	Source
Respiratory CO_2 [1]	Global	40	after Jahnke (1996)
		61	after Christensen (2000)
		60-75	Wenzhöfer and Glud (2002)
		43	Seiter et al. (2005)
Calcite Dissolution	Global	27-54	Archer (1996b)
	Global	22-81	Hensen et al. (2003)
	Global	13	Milliman (1999)
Alkalinity / TCO_2	Pacific	55	Berelson et al (1994)
	Indo-Pacific	91	Berelson et al (1994) [2]
	Global	100	after Berelson et al (1994)
		120	after Berelson et al (1994) [2]
		120	Mackenzie et al. (1993)
		100	Summary, this study
DOC	Atlantic [3]	4	Otto (1996)
	Global [3]	18	Otto (1996)
Total C	Global	120	Summary, this study

[1] Estimated as oxic respiration of organic matter.
[2] Using data of Broecker and Peng (1987).
[3] Including water depth above 1000 m.

water saturation conditions the global estimate extending the Berelson et al. (1994) approach is in agreement to that of Mackenzie et al. (1993). Based on Eq. 9.22 and assuming an total mineralization of $55 \cdot 10^{12}$ mol C yr^{-1} as well as an average contribution of $15 \cdot 10^{12}$ mol yr^{-1} from non-respiratory dissolution (Archer 1996b) we may come up with a total alkalinity flux of about $100 \cdot 10^{12}$ mol yr^{-1} as a best current estimate.

In combination with the flux of dissolved organic carbon (DOC), which may add another $20 \cdot 10^{12}$ mol yr^{-1} (Otto 1996; Table 9.7), a total carbon release from deep-sea sediments of about $120 \cdot 10^{12}$ mol yr^{-1} seems to be the best recent approximation regarding all sources of uncertainty.

Summary

The main subjects addressed in Chapter 9 are listed below:

- The major site of marine carbonate accumulation is the neritic environment, including coral reefs, banks and continental shelves, and pelagic calcite-rich sediments. In total, about $35 \cdot 10^{12}$ mol $CaCO_3$ accumulate per annum in the marine realm.

- Based on budget calculations of calcium carbonate, reservoir sizes in the world ocean and exchange fluxes between reservoirs the carbonate system is not in steady state.

- However, calcium carbonate budget calculations are strongly biased by inexact estimations of calcite production in the surface ocean and of the dissolution of pelagic biogenic calcite in the water column and in sediments above the calcite lysocline. In addition, the uncertainty is enhanced by the difficulty to estimate dissolved inorganic carbon release from sediments.

- The total carbon release from deep-sea sediments is estimated to be about $120 \cdot 10^{12}$ mol yr^{-1}, but is subject to great uncertainty due to the complexity of processes controlling carbon remobilization.

- Both bottom water undersaturation and organic matter decay are responsible for calcium carbonate dissolution in the sediments at more or less equal levels.

- The efficiency of calcium carbonate dissolution by metabolic CO_2 strongly depends on the organic carbon / calcium carbonate rain ratio at the sediment surface, the oxidation rate of organic matter (and the depth horizon, where oxidation occurs), as well as the saturation state of bottom water (Ω) and the dissolution rate constant k_d.

9.5 Problems

Problem 1

Where would you expect more $CaCO_3$ production: On the continental shelves, on the slopes, or in the deep sea?

Problem 2

Explain the difference between $CaCO_3$ production and $CaCO_3$ accumulation. Discuss the difference between both in connection with the processes of $CaCO_3$ dissolution in the water column and in sediment.

Problem 3

At which water depth would you expect the calcite compensation depth (CCD) in waters of high latitudes and in which water depth in waters of low latitudes? Explain your answer.

Problem 4

Which carbonate species has the highest concentrations in sea-water? How much of the total calcium concentration in normal sea-water exists as $CaSO_4$ complex? Under which conditions is this complex rather insignificant in anoxic pore-water?

Problem 5

$CaCO_3$ dissolution fluxes from sediment to ocean bottom water can be estimated from C_{org} mineralization rates. What are the geochemical processes behind this correlation? Which calcite dissolution rate would you expect for sediments in an upwelling area, and which for deep-sea sediments?

References

Adler, M., Hensen, C., Kasten, S. and Schulz, H.D., 2000. Computer simulation of deep-sulfate reduction in sediments off the Amazon Fan. International Journal of Earth Sciences (Geol. Rdsch.), 88: 619-629.

Adler, M., Hensen, C., Wenzhöfer, F., Pfeifer, K. and Schulz, H.D., 2001. Modeling of calcite dissolution by oxic respiration in supralysoclinal deep-sea sediments. Marine Geology, 177: 167-189.

Andersen, N.R. and Malahoff, A., 1977. The fate of fossil fuel CO2 in the Oceans. Plenum Press, NY, 749 pp.

Archer, D.E., 1991. Modeling the calcite lysocline. Journal of Geological Research, 96: 17037-17050.

Archer, D. and Maier-Reimer, E., 1994. Effect of deep-sea sedimentary calcite preservation on atmospheric CO2 concentration. Nature, 367: 260-263.

Archer, D.E., 1996a. An atlas of the distribution of calcium carbonate in sediments of the deep sea. Global Biochemical Cycles, 10: 159-174.

Archer, D.E., 1996b. A data-driven model of the global calcite lysocline. Global Biochemical Cycles, 10: 511-526.

Berelson, W.M., Hammond, D.E. and Cutter, G.A., 1990. In situ measurements of calcium carbonate dissolution rates in deep-sea sediments. Geochimica et Cosmochimica Acta, 54: 3013-3020.

Berelson, W.M., Hammond, D.E., McManus, J. and Kilgore, T.E., 1994. Dissolution kinetics of calcium carbonate in equatorial Pacific sediments. Global Biogeochemical Cycles, 8: 219-235.

Berger, W.H., 1976. Biogenic deep-sea sediments: Production, preservation and interpretation. In: Riley, J.P. and Chester, R. (eds) Chemical Oceanography, 5, Academic Press, London, pp. 266-388.

Berger, W.H., 1982. Increase of carbon dioxide in the atmosphere during deglaciation: The coral reef hypothesis. Naturwissenschaften, 69, 87.

Broecker, W.S. and Peng, T.-H., 1982. Tracers in the Sea. Lamont-Doherty Geol. Observation, Eldigo Press, Palisades, NY, 690 pp.

Broecker, W.S. and Peng, T.-H., 1987. The Role of CaCO3 compensation in the glacial to interglacial atmospheric CO2 change. Global Biogeochemical Cycles, 1: 15-29.

DeBaar, H.J.W. and Suess, E., 1993. Ocean carbon cycle and climate change - An introduction to the interdisciplinary Union Symposium. Global and Planetery Change, 8: VII-XI.

Dittert, N., Baumann, K.H., Bickert, T., Henrich, R., Huber, R., Kinkel, H., Meggers, H. and Müller, P., 1999. Carbonate dissolution in the Deep-Sea: Methods, quantification and paleoceanography application. In: Fischer, G. and Wefer, G. (eds) Use of proxies in paleoceanography: examples from the South Atlantic, Springer, Berlin, Heidelberg, 255-284.

Emerson, S.R., Jahnke, R., Bender, M., Froelich, P., Klinkhammer, G., Bowser, C. and Setlock, G., 1980. Early diagenesis in sediments from the eastern equatorial Pacific. 1. Pore water nutrient and carbonate results. Earth Planet Science Letters, 49: 57-80.

Emerson, S. and Bender, M., 1981. Carbon fluxes at the sediment-water interface of the deep-sea: calcium carbonate preservation. Journal of Marine Research, 39: 139-162.

Emerson, S., Grundmanis, V. and Graham, D., 1982. Carbonate chemistry in marine pore waters: MANOP sites C and S. Earth and Planetary Science Letters, 61: 220-232.

Feely, R.A., Sabine, C.L., Lee, K., Berelson, W., Kleypas, J., Fabry, V.J. and Millero, F.J., 2004. Impact of Anthropogenic CO_2 on the $CaCO_3$ System in the Oceans. Science, 305: 362-366.

Fischer, G., Wefer, G., Romero, O., Dittert, N., Ratmeyer, V. and Donner, B., 2004. Transfer of Particles into the Deep Atlantic and the Global Ocean. In: Wefer, G., Mulitza, S. and Ratmeyer, V. (eds) The South Atlantic in the Late Quaternary. Springer Berlin, Heidelberg, New York, pp. 21-46.

Freiwald, A., 2002. Reef-forming cold-water corals. In: Wefer, G., Billet, D., Hebbeln, D., Jørgensen, B.B., Schlüter, M., and Van Weering, T. (eds) Ocean margin systems, Springer, Berlin, Heidelberg, 365-385.

Goyet, C. and Poisson, A., 1989. New determination of carbonic acid dissociation constants in seawater as a function of temperature and salinity. Deep-Sea-Research, 36: 1635-1654.

Hales, B. and Emerson, S., 1996. Calcite dissolution in sediments of the Ontong-Java Plateau: In situ measurements of pore water O2 and pH. Global Biogeochemical Cycles, 10: 527-541.

Hales, B. and Emerson, S., 1997a. Calcite dissolution in sediments of the Ceara Rise: In situ measurements of porewater O2, pH, and CO2(aq). Geochimica et Cosmochimica Acta, 61: 501-514.

Hales, B. and Emerson, S., 1997b. Evidence in support of first-order dissolution kinetics of calcite in seawater. Earth and Planetary Science Letters, 148: 317-327.

Hammond, D.E., McManus, J., Berelson, W.M., Kilgore, T.E. and Pope, R.H., 1996. Early diagenesis of organic material in equatorial Pacific sediments: stoichiometry and kinetics. Deep-Sea Research, 43: 1365-1412.

Hay, W.W. and Southam, J.R., 1977. Modulation of marine sedimentation by continental shelves. In: Andersen, N.R. and Malahoff, A. (eds) The fate of fossil fuel CO2 in the Oceans. Plenum Press, NY, pp. 564-604.

Hensen, C., Landenberger, H., Zabel, M., Gundersen, J.K., Glud, R.N. and Schulz, H.D., 1997. Simulation of early diagenetic processes in continental slope sediments in Southwest Africa: The computer model CoTAM tested. Marine Geology, 144: 191-210.

Hensen, C., Landenberger, H., Zabel, M. and Schulz, H.D., 1998. Quantification of diffusive benthic fluxes of nitrate, phosphate and silicate in the Southern Atlantic Ocean. Global Biogeochemical Cycles, 12: 193-210.

Jahnke, R.A., Craven, D.B. and Gaillard, J.-F., 1994. The influence of organic matter diagenesis on CaCO3 dissolution at the deep-sea floor. Geochimica et Cosmochimica Acta, 58: 2799-2809.

Jahnke, R.A., 1996. The global ocean flux of particulate

organic carbon: Areal distribution and magnitude. Global Biogeochemical Cycles, 10: 71-88.

Jahnke, R.A., Craven, D.B., McCorkle, D.C. and Reimers, C.E., 1997. CaCO3 dissolution in California continental margin sediments: The influence of organic matter remineralization. Geochimica et Cosmochimica Acta, 61: 3587-3604.

James, N.P. and Clarke, J.A.D., 1997. Cool-water carbonates, SEPM Spec. Publ., 56, Tulsa, Oklahoma, 440 pp.

Jansen, H., R.E., Z. and Wolf-Gladrow, D.A., 2002. Modeling the dissolution of settling CaCO3 in the Ocean. Glob. Biogeochem. Cycles, 16(2): 11, 1-16.Keir, R.S., 1983. Variation in the carbonate reactivity of deep-sea sediments: determination from flux experiments. Deep-Sea Res., 30(3A): 279-296.

Keir, R.S., 1980. The dissolution kinetics of biogenic calcium carbonates in seawater. Geochimica et Cosmochimica Acta, 44: 241-252.

Kharaka, Y.K., Gunter, W.D., Aggarwal, P.K., Perkins, E.H. and DeBraal, J.D., 1988. SOLMINEQ88: a computer program for geochemical modeling of water-rock-interactions. Water-Resources Invest. Report, 88-4227, US Geol. Surv., 207 pp.

Lindberg, B. and Mienert, J., 2005. Postglacial carbonate production by cold-water corals on the Norwegian Shelf and their role in the global carbonate budget. Geology, 33(7): 537-540, doi: 10.1130/G21577.1.

Lisitzin, A.P., 1996. Oceanic sedimentation: Lithology and Geochemistry (English Translation edited by Kennett, J.P.). Amer. Geophys. Union, Washington, D.C., 400 pp.

Luff, R., Wallmann, K., 2003. Fluid flow, methane fluxes, carbonate precipitation and biogeochemical turnover in gas hydrate-bearing sediments at Hydrate Ridge, Cascadia Margin: Numerical modeling and mass balances. Geochim. Cosmochim. Acta 67 (18), 3403-3421.

Luff, R., Wallmann, K., Aloisi, G., 2004. Numerical modeling of carbonate crust formation at cold vent sites: significance for fluid and methane budgets and chemosynthetic biological communities. Earth Planet. Sci. Lett. 221, 337-353.

Mackenzie, F.T., Ver, L.M., Sabine, C., Lane, M. and Lerman, A., 1993. C, N, P, S global biogeochemical cycles and modeling of global change. In : Wollast, R., Mackenzie, F.T. and Chou, L. (eds), Interactions of C, N, P and S biogeochemical cycles and global change. NATO ASI Series, 14, Springer Verlag, pp 1-61.

Maier-Reimer, E. and Bacastow, R., 1990. Modelling of geochemical tracers in the ocean. Climate-Ocean Interaction. In: Schlesinger, M.E. (ed), Climate-ocean interactions, Kluwer, pp. 233-267.

Martin, W.R. and Sayles, F.L., 1996. CaCO3 dissolution in sediments of the Ceara Rise, western equatorial Atlantic. Geochimica et Cosmochimica Acta, 60: 243-263.

Mehrbach, C., Culberson, C., Hawley, J.E. and Pytkowicz, R.M., 1973. Measurement of the apparent dissociation constants of carbonic acid in seawater at atmospheric pressure. Limnology and Oceanography, 18: 897-907.

Millero, F.J., 1995. Thermodynamics of the carbon dioxide systems in the oceans. Geochimica et Cosmochimica Acta, 59: 661-677.

Milliman, J.D., 1993. Production and accumulation of calcium carbonate in the ocean: budget of a nonsteady state. Global Biogeochemical Cycles, 7: 927-957.

Milliman, J.D. and Droxler, A.W., 1996. Neritic and pelagic carbonate sedimentation in the marine environment: ignorance is not a bliss. Geologische Rundschau, 85: 496-504.

Milliman J. D., Troy P. J., Balch W. M., Adams A. K., Li Y.-H., and Mackenzie F. T., 1999. Biologically mediated dissolution of calcium carbonate above the chemical lysocline? Deep-Sea Res. I 46, 1653–1669.

Morse, J.W., 1978. Dissolution kinetics of calcium carbonate in sea water: VI. The near-equilibrium dissolution kinetics of calcium carbonate-rich deep-sea sediments. American Journal of Science, 278: 344-353.

Morse, J.W. and Berner, R.A., 1979. Chemistry of calcium carbonate in the deep ocean. In: Jenne, E.A. (ed), Chemical modelling in aqueous systems. Am. Chem. Soc., Symp. Ser., 93, pp. 499-535.

Morse, J.W. and Mackenzie, F.T., 1990. Geochemistry of sedimentary carbonates. Elsevier, Amsterdam, 707 pp.

Mucci, A., Sundby, B., Gehlen, M., Arakaki, T., Zhong, S., Silverberg, N., 2000. The fate of carbon in continental shelf sediments of eastern Canada: a case study. Deep-Sea Res. II 47, 733-760.

Murray, J.W., 1897. On the distribution of the pelagic foraminifera at the surface and on the sea floor of the ocean. Nat. Sci., 11: 17-27.

Murray, J.W., Emerson, S. and Jahnke, R.A., 1980. Carbonate saturation and the effect of pressure on the alkalinity of interstitial waters from the Guatemala Basin. Geochimica et Cosmochimica Acta, 44: 963-972.

Nordstrom, D.K., Plummer, L.N., Wigley, T.M.L., Wolery, T.J., Ball, J.W., Jenne, E.A., Basset, R.L., Crerar, D.A., Florence, T.M., Fritz, B., Hoffman, M., Holdren, G.R. Jr., Lafon, G.M., Mattigod, S.V. McDuff, R.E., Morel, F., Reddy, M.M., Sposito, G. and Thrailkill, J., 1979. A comparision of computerized chemical models for equilibrium calculations in aqueous systems. In: Jenne, E.A. (ed), Chemical modeling in aqueous systems, speciation, sorption, solubility, and kinetics, 93, American Chemical Society, pp. 857-892.

Opdyke, B.D. and Walker, J.C.G., 1992. Return of the coral reef hypothesis: basin to shelf partitioning of CaCO3 and its effects on atmospheric CO2. Geology, 20: 733-736.

Orr, J.C., Fabry, V.J., Aumont, O., Bopp, L., Doney, S.C., Feely, R.A., Gnanadesikan, A., Gruber, N., Ishida, A., Joos, F., Key, R.M., Lindsay, K., Maier-Reimer, E., Matear, R., Monfray, P., Mouchet, A., Najjar, R.G., Plattner G.-K., Rodgers, K.B., Sabine, C.L., Sarmiento, J.L., Schlitzer, R., Slater, R.D., Totterdell, I.J., Weirig, M.-F., Yamanaka, Y. and Yool, A., 2005. Anthropogenic ocean acidification over the twenty-first century and its impact on calcifying organisms. Nature 437: 681-686, doi:10.1038/nature04095.

Otto, S., 1996. Die Bedeutung von gelöstem organischen Kohlenstoff (DOC) für den Kohlenstoffffluß im Ozean. Berichte, 87, Fachbereich Geowissenschaften, Universität Bremen, 150 pp.

Palmer, A.N., 1991. The origin and morphology of limestone caves. Geological Society American Bulletin, 103: 1-21.

Parkhurst, D.L., Thorstensen, D.C. and Plummer, L.N., 1980. PHREEQE - a computer program for geochemical calculations. Water-Resources Invest. Report, 80-96, US Geol. Surv., 219 pp.

Parkhurst, D.L., 1995. User's guide to PHREEQC: a computer model for speciation, reaction-path, advective-transport, and inverse geochemical calculation. Water-Resources Invest. Report, 95-4227, US Geol. Surv., 143 pp.

Pfeifer, K., Hensen, C., Adler, M., Wenzhöfer, F., Weber, B. and Schulz, H.D., 2002. Modeling of subsurface calcite dissolution, including the respiration and reoxidation processes of marine sediments in the region of equatorial upwelling off Gabon. Geochim. Cosmochim. Acta, 66(24): 4247-4259.

Plummer, L.N., Wigley, T.M.L. and Parkhurst, D.L., 1978. The kinetics of calcite dissolution in CO2-water systems at 5°C to 60°C and 0.0 to 1.0 atm CO2. Am. J. Sci., 278: 179-216.

Plummer, L.N., Wigley, T.M.L. and Parkhurst, D.L., 1979. Critical review of the kinetics of calcite dissolution and precipitation. In: Jenne, E.A. (ed), Chemical modelling in aqueous systems. Am. Chem. Soc., Symp. Ser., 93, pp. 537-572.

Raiswell, R., Fisher, Q.J. (2004) Rates of carbonate cementation associated with sulphate reduction in DSDP/ODP sediments: implications for the formation of concretions. Chem. Geol. 211, 71-85.

Redfield, A.C., 1958. The biological control of chemical factors in the environment. Am. Scientist, 46: 206-2226.

Reimers, C.E., Jahnke, R.H. and McCorkle, D.C., 1992. Carbon fluxes and burial rates over the continental slope and rise off central California with implications for the global carbon cycle. Global Biogeochemical Cycles, 6: 199-224.

Roberts, H.H. and Macintyre, I.G. (eds), 1988. Special issue: Halimeda. Coral Reefs, 6(3/4), 121-280.

Roy, R.N., Roy, L.N., Vogel, K.M., Moore, C.P., Pearson, T., Good, C.E., Millero, F.J. and Campbell, D.M., 1993. Determination of the ionization constance of carbonic acid in seawater. Marine Chemistry, 44: 249-268.

Seiter, K., Hensen, C. and Zabel, M., 2005. Benthic carbon mineralization on a global scale. Glob. Biogeochem. Cycles, 19: GB1010, doi:10.1029/2004GB002225.

Siegenthaler, H.H. and Wenk, T., 1984. Rapid atmospheric CO2 variations and ocean circulation. Nature, 308: 624-626.

Sundquist, E.T. and Broeker, W.S., 1985. The carbon cycles and atmospheric CO2: natural variations archean to present. American Geophysical Union, Washington, D.C., 627 pp.

Svensson, U. and Dreybrodt, W., 1992. Dissolution kinetics of natural calcite minerals in CO2-water systems approaching calcite equilibrium. Chemical Geology, 100: 129-145.

Takahashi, T., Broecker, W.S., Bainbridge, A.E. and Weiss, R.F., 1980. Carbonate chemistry of the Atlantic, Pacific and Indian Oceans: The results of the Geosecs expeditions, 1972-1978, Natl. Sci. Found., Washington D. C.

Vecsei, A., 2004. A new estimate of global reefal carbonate production including fore-reefs. Global and Planetary Change, 43: 1-18.

Wenzhöfer, F., Adler, M., Kohls, O., Hensen, C., Strotmann, B., Boehme, S. and Schulz, H.D., 2001. Calcite dissolution driven by benthic mineralization in the deep-sea: *in situ* measurements of Ca^{2+}, pH, pCO_2, O_2. Geochim. Cosmochim. Acta, 65(16): 2677-2690.

Wolf-Gladrow, D., 1994. The ocean as part of the global carbon cycle. Environ. Sci. & Pollut. Res., 1: 99-106.

Wollast, R., 1994. The relativ importance of biomineralisation and dissolution of CaCO3 in the global carbon cycle. In: Doumenge, F., Allemand, D. and Toulemont, A. (eds), Past and present biomineralisation processes: Considerations about the carbonate cycle. Bull. de l'Institute océanographique, 13, Monaco, pp. 13-35.

Zeebe, R.E. and Wolf-Gladrow D.A., 2001. CO_2 in Seawater: Equilibrium, Kinetics, Isotopes. Elsevier Oceanography Series, 65, 346 pp.